

# Advanced NOMA Assisted Semi-Grant-Free Transmission Schemes for Randomly Distributed Users

Huabing Lu, *Student Member, IEEE*, Xianzhong Xie, *Member, IEEE*,  
 Zhaoyuan Shi, *Student Member, IEEE*, Hongjiang Lei, *Senior Member, IEEE*,  
 Helin Yang, *Member, IEEE*, and Jun Cai, *Senior Member, IEEE*

## Abstract

Non-orthogonal multiple access (NOMA) assisted semi-grant-free (SGF) transmission has recently received much research attention, which can serve the grant-free (GF) users with the grant-based (GB) users' spectrum. In this paper, we first extend the SGF scheme with the best user scheduling (BU-SGF) to a more practical randomly deployed users system. Then, a cumulative distribution function (CDF)-based scheduling aided SGF (CS-SGF) scheme is proposed to ensure fair admission probability for all GF users. Meanwhile, we analytically demonstrate that, for both BU-SGF and CS-SGF schemes, full diversity orders can be achieved only when the served users' data rate is capped. To address this issue, we propose an efficient power control strategy to relax such data rate constraint and further enhance the outage probability. In addition, after applying the proposed power control strategy, both schemes' outage performances are analyzed by utilizing stochastic geometry. Theoretic and simulation results demonstrate that, with the proposed power control strategy both schemes can achieve full diversity orders in all cases.

**Index Terms** —NOMA, CDF-based scheduling, outage probability, fairness, semi-grant-free transmission.

H. Lu, X. Xie, and Z. Shi are with the School of Computer Science and Technology, Chongqing University of Posts and Telecommunications, Chongqing 400065, China (e-mail: [huabing\\_lu@stu.cqupt.edu.cn](mailto:huabing_lu@stu.cqupt.edu.cn), [xiexzh@cqupt.edu.cn](mailto:xiexzh@cqupt.edu.cn), [shizy@stu.cqupt.edu.cn](mailto:shizy@stu.cqupt.edu.cn)).

H. Lei is with the School of Communication and Information Engineering, Chongqing University of Posts and Telecommunications, Chongqing 400065, China, also with Chongqing Key Lab of Mobile Communications Technology, Chongqing 400065, China, and also with Shaanxi Key Laboratory of Information Communication Network and Security, Xi'an University of Posts and Telecommunications, Xi'an, Shaanxi 710121, China (e-mail: [leihj@cqupt.edu.cn](mailto:leihj@cqupt.edu.cn)).

H. Yang is with the School of Computer Science and Engineering, Nanyang Technological University, Singapore 639798 (e-mail: [hyang013@e.ntu.edu.sg](mailto:hyang013@e.ntu.edu.sg)).

J. Cai is with the Network Intelligence and Innovation Lab (NI<sup>2</sup>L), Department of Electrical and Computer Engineering, Concordia University, Montreal, QC H3G 1M8, Canada (e-mail: [jun.cai@concordia.ca](mailto:jun.cai@concordia.ca)).

## I. INTRODUCTION

Three important use cases, namely, enhanced Mobile Broadband (eMBB), Ultra Reliable Low Latency Communications (URLLC) and massive Machine Type Communications (mMTC), have been standardized for the fifth-generation mobile communication systems [1], [2]. Each use case has its unique characteristics. Specifically, eMBB mainly focuses on human-oriented applications, and aims to further improve the communication throughput and capacity, while URLLC and mMTC seek to connect billions of Internet of Things (IoT) devices to the Internet. URLLC focuses on mission-critical applications, where unprecedented levels of reliability and latency are of the utmost importance. In contrast, mMTC aspires to connect a huge number of smart devices to the Internet [3].

Different from human type applications where the transmitted packages are always quite long, short packets are common for the traffic generated by IoT devices [4]–[6]. However, conventional mobile communication systems operate on grant-based (GB) protocols, namely, each communication device first transmits a scheduling request to the base station (BS) and then the BS sends a grant back for resource allocation, which are not designed for short-packet transmission. If adopting GB protocols for IoT transmissions, the lengthy handshaking process of requesting for grant will be prohibitively costly for the signaling overhead and unacceptable for the resultant latency [7], [8].

Grant-free (GF) transmission is an effective way to tackle this problem, where the aforementioned request-grant process is omitted and dedicated resource blocks are reserved for these IoT devices to transmit whenever the packets arrive [8]–[11]. As the lengthy handshaking process is totally omitted, the transmission delay resulting from random access in conventional systems is eliminated and the spectrum efficiency can be improved. However, without central access control of the BS, collisions may frequently occur in GF transmission with lots of IoT devices, since the spectrum reserved for GF transmission is ordinarily limited and it is inevitable that multiple users will choose the same resource. To alleviate this situation, some studies integrated non-orthogonal multiple access (NOMA) with GF transmission, by which multiple devices' signals could be transmitted at the same resource but with different power levels or codebooks [12]–[14]. However, in systems with enormous devices, the number of devices may still exceed the NOMA capability for successful decoding, which deteriorates the system performance [14].

Recently, NOMA assisted semi-grant-free (SGF) transmission schemes, which encourage GB

users to share their resources to delay tolerant IoT devices with short transmission packets have received much research attention [14], [15]. In SGF transmission schemes, some IoT devices with delay-tolerant packets can be bypassed with GB users' resources, so as to reduce the number of devices that content for the resources reserved for GF transmissions. Hence, the successful communication probability for the latency-critical IoT devices could be improved. Compared to GB transmission lower signaling overhead is needed in SGF transmission, meanwhile the collision event is effectively managed compared with pure GF transmission [15].

### A. Related Work

In recent years, extensive studies have investigated various aspects of NOMA transmission schemes based on either pure GB or pure GF protocols. To be specific, for pure GB NOMA, Zhang *et al.* [16] proposed a power backoff scheme for uplink NOMA. Yang *et al.* [17] developed a power allocation scheme to guarantee the performance gain of NOMA to conventional orthogonal multiple access (OMA) scheme. By utilizing stochastic geometry, the outage performances and/or ergodic data rates of different NOMA schemes were characterized in [18]–[22]. With respect to pure GF NOMA, most of the existing studies were designed based on code domain NOMA. By exploiting the sparsity of user activity in mMTC scenario, Wang *et al.* [23] proposed a low complexity multi-user detector based on structured compressive sensing. Du *et al.* [24] developed a block compressed sensing-based sparse signal recovery framework to improve the multi-user detection performance. Abbas *et al.* [25] proposed a novel and generalized framework for massive GF-NOMA scheme. Wei *et al.* [26] devised a message-passing receiver for sparse code multiple access systems. For more comprehensive review of GB/GF NOMA, we refer the readers to [27]–[31] and the references therein.

Till now, several studies have investigated the NOMA-assisted SGF transmission schemes [15], [32]–[36]. Specifically, the concept of SGF scheme was firstly proposed in [15], where two SGF mechanisms were developed to effectively restrict the number of admitted GF users and ensure that the admission of the GF users do not cause too much performance degradation to the GB users. Jayanth *et al.* [32] used cognitive radio principles to manage the interference from GF users to GB users. Zhang *et al.* [33], [34] developed a dynamic protocol to provide an accurate access threshold for the admission of the GF users. Note that, the spatial effect of users' deployment was investigated in [33], [34], where stochastic geometry was employed to analyze the outage performance [33] and ergodic rates [34]. Yang *et al.* [35] proposed an adaptive power

allocation strategy for the GB user to relieve performance impairment due to the admission of GF users. However, in all these studies, pre-fixed successive interference cancellation (SIC) decoding orders were assumed, which led to outage probability error floors for the GB or GF users. In order to avoid such error floors, Ding *et al.* [36] proposed a new SGF scheme by resorting to hybrid successive interference cancellation (HSIC) [37], which could guarantee the performance of the GB users to be same as that with OMA. It means that the admission of GF users will effectively improve the spectrum efficiency without affecting the GB users' performance.

### *B. Motivation and Contributions*

Even though the aforementioned work has done some novel studies on NOMA-assisted SGF transmission schemes. Three critical problems are still waiting for solution: 1) Only small scale fading (Rayleigh fading) was investigated in [15], [35], [36], and the impact of users' locations was ignored. Although Path loss was considered in [32], only homogeneous user locations (the distances of all GF users to the BS are the same) was investigated. [33] and [34] discussed the impact of user locations. However, random user selection was investigated, which failed to exploit multiuser diversity; 2) All the existing SGF schemes preferred to schedule the GF users with strongest or weakest channel gains. This leads to the fairness problem, since the users close to the BS or cell boundary may be scheduled more frequently.<sup>1</sup> Therefore, it is necessary to address this fairness issue for practical SGF communication systems; 3) The robust transmission of the GF users (namely, the GF users can achieve non-zero diversity orders) can be achieved only in the case of limited target rate pairs [36]. There is necessary to develop a SGF scheme which can guarantee robust transmission in all cases.

Motivated by the previous discussions, this paper dedicates to develop new SGF schemes that can be applied in systems with randomly deployed users, and analyze the corresponding outage performance. The main contributions of this paper are outlined as follows:

- To study the spatial effect of user locations, we consider the SGF scheme with the best user scheduling (BU-SGF) [36], namely, the GF user with the maximal data rate will be scheduled, in systems with randomly deployed users. Compared to [36], where only Rayleigh fading is studied, the considered scenario is more practical and more challenging.

<sup>1</sup>In general, fairness in user scheduling can be divided into two categories [38]: throughput-based fairness and resource-based fairness. This paper focuses on resource-based fairness, namely, the GF users with different distances to the BS have an equal probability in scheduling.

- We propose a fair scheduling scheme for SGF transmission systems by invoking cumulative distribution function (CDF)-based scheduling (CS-SGF) [38], [39]. Compared to the random selection SGF scheme in [33], [34], the CS-SGF scheme can effectively exploit multi-user diversity.
- For both BU-SGF and CS-SGF schemes, the admitted GF users' outage probabilities are analytically analyzed by applying stochastic geometry. Moreover, we derive the rate constraints under which both schemes can achieve full diversity orders, or zero diversity orders.
- We propose a power control strategy to enhance the admitted GF users' outage performance without introducing extra signaling overhead. In addition, the proposed strategy can be executed distributedly.
- Theoretical analyses of the admitted GF users' outage probabilities are developed for both BU-SGF and CS-SGF schemes with the proposed power control strategy. To get more insights, we also analyze the asymptotic outage probabilities and the achievable diversity orders. Results demonstrate that the proposed power control strategy can not only improve the outage performance, but also effectively eliminate the rate constraints for achieving full diversity orders.

### *C. Organization*

The rest of this paper is organized as follows. Section II introduces the system model. Two SGF transmission schemes are presented in Section III. In Section IV, the outage performances of the two schemes are analyzed. Section V proposes the power control strategy and analyzes the outage performances of the two schemes after applying the power control strategy. In Section VI, simulation results are presented to verify the theoretical analyses and Section VII concludes this paper.

## II. SYSTEM MODEL

In this section, the signal model is presented first, then the decoding scheme with HSIC is introduced.

### *A. Signal Model*

A single-cell uplink cellular network is considered, where the BS is located at the center of the coverage disc area with radius  $D$ . Similar to [15], [35], [36], we assume that there are  $K$  GF users and one GB user, where these GF users are randomly distributed in the disc area  $\mathcal{D}_F$  with radius  $D_F$  ( $D_F \leq D$ ), and the GB user (denoted as  $U_B$ ) randomly deployed in a ring region

$\mathcal{D}_B$  with inner radius  $D_0$  ( $D_0 > 0$ ) and outer radius  $D_1$  ( $D_1 \leq D$ ). The location distribution of the GF users is modeled as a homogeneous Binomial point process (HBPP)  $\Upsilon_F$  [40]. We also assume that the GB user communicates with the BS in conventional grant-based protocol and has been allocated one dedicated resource block, so that the channel state information (CSI) of the GB user is known to the BS [34].

We consider a composite channel model with both quasi-static Rayleigh fading and large scale path loss, where the channel coefficients are assumed to be invariant during each transmission block and change independently between blocks. The channel between the  $k$ -th ( $k \in \{1, \dots, K\}$ ) GF user  $U_k$  and the BS is modeled as  $h_k = \frac{\zeta_k}{\sqrt{1+r_k^\alpha}}$ , where  $r_k$  represents the distance between  $U_k$  and the BS,  $\alpha$  denotes the path loss exponent, and  $\zeta_k$  represents Rayleigh fading coefficient with  $\zeta_k \sim \mathcal{CN}(0, 1)$ . Without loss of generality, we assume that the GF users' channel gains are ordered as

$$|h_1|^2 \leq \dots \leq |h_K|^2. \quad (1)$$

Note that, this assumption is used to facilitate the performance analysis, and all nodes in the system do not know this order [36]. Similarly, the channel of  $U_B$  to the BS is defined as  $g = \frac{\zeta_B}{\sqrt{1+r_B^\alpha}}$ , where  $\zeta_B \sim \mathcal{CN}(0, 1)$  and  $r_B$  denotes the distance between  $U_B$  and the BS. Every user can estimate its CSI by exploiting pilot signals sent by the BS.

Based on these assumptions, the CDFs of the unordered channel gains of the GF and GB users can be respectively expressed as [18], [41]

$$F_F(x) = \frac{2}{D_F^2} \int_0^{D_F} [1 - e^{-(1+r^\alpha)x}] r dr \stackrel{(a)}{\approx} \frac{1}{2} \sum_{l=1}^L \Psi_l (1 - e^{-\mu_l x}), \quad (2)$$

$$F_B(y) = \frac{2}{D_1^2 - D_0^2} \int_{D_0}^{D_1} [1 - e^{-(1+r^\alpha)y}] r dr \stackrel{(b)}{\approx} \frac{1}{D_1 + D_0} \sum_{n=1}^N \Phi_n (1 - e^{-c_n y}), \quad (3)$$

where both (a) and (b) are obtained by applying Gaussian-Chebyshev quadrature [42],  $\psi_l = \cos\left(\frac{2l-1}{2L}\pi\right)$ ,  $\mu_l = 1 + \left(\frac{D_F}{2} + \frac{D_F}{2}\psi_l\right)^\alpha$ ,  $\Psi_l = \frac{\pi}{L}\sqrt{1-\psi_l^2}(1 + \psi_l)$ ,  $\varphi_n = \cos\left(\frac{2n-1}{2N}\pi\right)$ ,  $\phi_n = \frac{D_1+D_0}{2} + \frac{D_1-D_0}{2}\varphi_n$ ,  $\Phi_n = \frac{\pi}{N}\sqrt{1-\varphi_n^2}\phi_n$ ,  $c_n = 1 + \phi_n^\alpha$ ,  $L$  and  $N$  are parameters for ensuring complexity-accuracy tradeoff. From (3), we can derive the probability density function (pdf) of  $U_B$ 's channel gain as

$$f_B(y) \approx \frac{1}{D_1 + D_0} \sum_{n=1}^N \Phi_n c_n e^{-c_n y}. \quad (4)$$

One GF user<sup>2</sup> (denoted as  $U_F \in \{U_1, \dots, U_K\}$ ) will be admitted for transmission using the resource block allocated to  $U_B$  after distributed contention<sup>3</sup>, where the contention criteria will be introduced in Section III. Therefore, the signal received at the BS can be expressed as

$$y = h\sqrt{P_F} s_F + g\sqrt{P_B} s_B + n_0, \quad (5)$$

where  $s_F$  and  $s_B$  denote the transmitted symbols of  $U_F$  and  $U_B$ , respectively.  $P_F$  ( $P_B$ ) represents the transmit power of  $U_F$  ( $U_B$ ),  $h$  ( $h \in \{h_1, \dots, h_K\}$ ) denotes the channel of  $U_F$ , and  $n_0$  represents the additive white Gaussian noise (AWGN) with zero mean and variance  $\sigma^2 = 1$ . To facilitate the theoretical analysis, we assume that all the GF users have the same target data rate. Let  $R_B$  ( $R_F$ ) and  $\gamma_B = 2^{R_B} - 1$  ( $\gamma_F = 2^{R_F} - 1$ ) respectively represent the target data rate and the target signal-to-interference-plus-noise ratio (SINR) of  $U_B$  ( $U_F$ ). Assuming the maximal transmit powers of the GB and GF users are the same and denoted as  $P_m$ . The notations used in this paper are summarized in Table I.

### B. Decoding with HSIC

Prior to user scheduling, the BS will first broadcast a threshold, denoted as  $\tau_0 \triangleq \max \{0, \tau(|g|^2)\}$ , to all the GF users [36]. Here,  $\tau(|g|^2) = \frac{P_B|g|^2}{\gamma_B} - 1$ , and it is derived based on the condition that the BS can correctly decode  $U_B$ 's signal at the first stage of SIC, namely,  $\log \left(1 + \frac{P_B|g|^2}{\tau(|g|^2)+1}\right) \geq R_B$ . HSIC is employed in the decoding process, as it can effectively avoid outage error floors [37].

If the effective received power of  $U_F$ 's signal is larger than  $\tau_0$  (namely,  $P_F|h|^2 > \tau_0$ ), the BS will decode  $U_F$ 's signal first, with a data rate  $R_F^{\text{fs}} = \log \left(1 + \frac{P_F|h|^2}{P_B|g|^2+1}\right)$ . Obviously, for the opposite decoding order,  $U_B$ 's signal cannot be successfully decoded, since  $P_F|h|^2 > \tau_0$  leads to  $\log \left(1 + \frac{P_B|g|^2}{P_F|h|^2+1}\right) < R_B$  and  $U_B$ 's data rate should be satisfied with priority. Then  $U_B$ 's signal will be decoded at the second stage of SIC, and after applying SIC, the data rate of  $U_B$  is  $\log (1 + P_B|g|^2)$ , which is the same as that achieved in OMA.

On the other hand, if  $P_F|h|^2 \leq \tau_0$ , the BS can decode  $U_B$ 's signal at either the first or the second stage of SIC. Accordingly,  $U_F$  will achieve a data of  $R_F^{\text{ss}} = \log (1 + P_F|h|^2)$  or

<sup>2</sup>Similar to [36], in this paper, we consider a single GF user is admitted to access the channel, while multiple users can be admitted by applying distributed scheduling [15].

<sup>3</sup>Distributed contention has been widely used in opportunistic carrier sensing [36], [43], [44], where the BS can schedule the most preferred user in a distributed manner. Take the strategy proposed in [44] as an example, which selects the user with the best channel condition to transmit. After estimating the CSI, each user selects a backoff time, e.g.,  $\pi_k$  for the  $k$ -th user, which is a unified mono-decreasing function of the channel gain. Once the contention time window (with duration  $\pi_0$ ) begins, the  $k$ -th user will send a flag to the BS after  $\pi_k$  ( $\pi_k < \pi_0$ ) expires. Thus, the user with the best channel will send its flag first and hence be identified to the BS.

TABLE I  
LIST OF NOTATIONS

| Notation                        | Description  |
|---------------------------------|--|
| $K$                             | Number of the grant free users   |
| $\mathcal{D}_F (\mathcal{D}_B)$ | Disc (ring) region distributed with GF (GB) users  |
| $D$                             | Coverage area of the BS  |
| $D_F$                           | Radius of the disc region $\mathcal{D}_F$  |
| $D_0 (D_1)$                     | Inner (outer) radius of the ring region $\mathcal{D}_B$  |
| $U_k$                           | The $k$ -th GF user ( $k \in \{1, \dots, K\}$ )  |
| $U_F$                           | The admitted GF user ( $U_F \in \{U_1, \dots, U_K\}$ )   |
| $U_B$                           | The GB user  |
| $R_F (R_B)$                     | Target rate of $U_F (U_B)$   |
| $\gamma_F (\gamma_B)$           | Target SINR of $U_F (U_B)$   |
| $\alpha_F (\alpha_B)$           | Target channel gain of $U_F (U_B)$ , $\alpha_F = \frac{\gamma_F}{P_F}$ , $\alpha_B = \frac{\gamma_B}{P_B}$ |
| $h_k$                           | Channel of $U_k$ with the BS   |
| $h (g)$                         | Channel of $U_F (U_B)$ with the BS   |
| $r_k$                           | Distance between $U_k$ and the BS  |
| $r_F (r_B)$                     | Distance between $U_F (U_B)$ and the BS  |
| $P_m$                           | Maximal transmit power of all users  |
| $P_k$                           | Transmit power of $U_k$  |
| $P_F (P_B)$                     | Transmit power of $U_F (U_B)$  |
| $\alpha$                        | Path loss exponent   |
| $f_X(\cdot)$                    | Probability density function (pdf) of $X$  |
| $F_X(\cdot)$                    | Cumulative distribution function of $X$  |
| $\mathbb{P}\{\cdot\}$           | Probability of an event  |
| $\triangleq$                    | Be defined as  |
| $f(a \mapsto b)$                | Replace $a$ in expression $f$ with $b$   |
| $\mathcal{CN}(\mu, \sigma^2)$   | Complex Gaussian random variable with mean $\mu$ and variance $\sigma^2$                                   |

$R_F^{\text{fs}} = \log \left( 1 + \frac{P_F |h|^2}{P_B |g|^2 + 1} \right)$ . Since  $R_F^{\text{ss}} > R_F^{\text{fs}}$ , in order to maximize  $U_F$ 's data rate, the BS will decode  $U_B$ 's signal first.

### III. SGF SCHEMES

In this section, we first extend the BU-SGF scheme [36] to systems with randomly deployed users, then the proposed CS-SGF scheme will be introduced. For ease of theoretical analysis, we assume that the GF users always transmit with the same fixed power  $P_F$  in both BU-SGF and CS-SGF schemes, namely,  $P_k = P_F$  for  $k \in \{1, \dots, K\}$ .

#### A. BU-SGF Scheme

In BU-SGF scheme [36], the GF user which can achieve the maximal data rate will be admitted to access  $U_B$ 's channel. The admission procedure consists of the following six steps:

- 1) The BS sends pilot signals.
- 2)  $U_B$  feedbacks its transmit power  $P_B$  and CSI  $g$  to the BS.
- 3) The BS calculates  $U_B$ 's decoding threshold  $\tau_0$ .
- 4) The BS broadcasts  $U_B$ 's effective received power  $P_B |g|^2$  and  $\tau_0$  to all GF users.

5)  $U_k$  calculates its transmit data rate, which is  $R_k^{\text{fs}} = \log \left( 1 + \frac{P_F |h_k|^2}{P_B |g|^2 + 1} \right)$  if  $P_F |h_k|^2 > \tau_0$ , or  $R_k^{\text{ss}} = \log (1 + P_F |h_k|^2)$  if  $P_F |h_k|^2 \leq \tau_0$ , where  $h_k$  denotes  $U_k$ 's transmit power. Note that, HSIC is applied here.

6) The GF user with the maximal data rate will be admitted to transmit through distributed contention (Thus, the contention criteria is each GF user's achievable data rate).

In BU-SGF scheme, the achievable rate of  $U_k$  ( $R_k^{\text{fs}}$  or  $R_k^{\text{ss}}$ ) is an increasing function of the channel gain  $|h_k|^2$ , so that the GF user closer to the BS will achieve a higher data rate with larger probability due to smaller path loss. Since the BU-SGF scheme always schedules the GF user with the maximal data rate, the GF user closer to the BS will be scheduled more frequently, and vice versa, which results in fairness issue among GF users. In the next subsection, we will propose a fair SGF scheme, which can schedule each GF user with equal probability.

### B. CS-SGF Scheme

We handle the fairness issue of SGF scheme by resorting to CDF-based scheduling, where the GF user with the largest CDF value about its channel gain, namely, the GF user whose channel is good enough relative to its own statistics, will be admitted [39], [41]. Since all the GF users' channels are independent with each other and their channel gains' CDF values are uniformly distributed in  $[0, 1]$  [38], each GF user has the same probability to have the largest CDF value and the admission fairness is guaranteed.

Assume that the CDF of  $U_k$ 's channel gain  $|h_k|^2$  is denoted as  $F_k(x)$ ,<sup>4</sup> which can be obtained by the user's long-term observation [38]. For Rayleigh small-scale fading, the CDF of  $U_k$ 's channel gain with a given distance  $r_k$  (the distance from  $U_k$  to the BS) can be expressed as

$$F_k(x|r_k) = 1 - e^{-(1+r_k^\alpha)x}. \quad (6)$$

At the beginning of each time slot, all GF users estimate their CDF values after estimating their own channels. By using distributed contention control strategy [44], the GF user with the largest CDF value can be admitted. The contention criteria is each GF user's CDF value, namely, each GF user's backoff time is set to be inversely proportional to its CDF value. Then, the admitted GF user  $U_F$  begins to transmit its signal with transmit power  $P_F$  over  $U_B$ 's resource block. According to [41] we have the following lemma, which gives the CDF of  $U_F$ 's channel gain for CS-SGF scheme.

<sup>4</sup>In this paper, we use "CDF" to denote the cumulative distribution function, e.g.,  $F_k(x)$ , and use "CDF value" to represent the corresponding output value of a CDF with a specific input  $x$ .

*Lemma 1:* The CDF of the scheduled GF user's channel gain for CS-SGF scheme can be expressed as

$$F_F(x) \approx \frac{1}{2} \sum_{l=1}^L \Psi_l (1 - e^{-\mu_l x})^K. \quad (7)$$

In the following two sections, the outage performance of the SGF schemes will be analyzed. Note that, in SGF scheme with HSIC, since  $U_B$  can always achieve the same performance as that in OMA, we only characterize  $U_F$ 's outage performance [36]. The main steps of the analysis procedure are listed as follows:

- 1) Derive  $U_F$ 's outage probability expressions.
- 2) Convert, combine, and/or simplify the outage probability expressions for easier calculation.
- 3) Calculate the exact approximation expressions for the outage probabilities by using the CDF/pdf expressions in (2), (3), (4), and (7).
- 4) Derive the high SNR approximations of the outage probabilities and the achieved diversity orders.

#### IV. PERFORMANCE ANALYSIS FOR SGF SCHEMES WITH FIXED TRANSMIT POWER

In this section,  $U_F$ 's outage probabilities and the achieved diversity orders will be derived for both CS-SGF and BU-SGF schemes.

##### A. Performance Analysis for BU-SGF Scheme

From Sections II and III, we can denote the outage probability of  $U_F$  for BU-SGF scheme by

$$\mathcal{P}_{BU} = \sum_{k=0}^K \mathbb{P} \left\{ E_k, \max\{R_i^{ss}, 1 \leq i \leq k\} < R_F, \max\{R_i^{fs}, k < i \leq K\} < R_F \right\}, \quad (8)$$

where  $E_k$  denotes the event that there are  $k$  users' effective received powers are less than  $U_B$ 's decoding threshold  $\tau_0$ .  $R_i^{fs} = \log(1 + \frac{P_F|h_i|^2}{P_B|g|^2 + 1})$  and  $R_i^{ss} = \log(1 + P_F|h_i|^2)$  represent the  $i$ -th GF user's achievable rate when its signal is decoded at the first and second stages of SIC, respectively.

As the GF users transmit with fixed power  $P_F$  (if admitted) and their channel gains are ordered as (1), the outage probability can be rewritten as

$$\mathcal{P}_{BU} = \mathbb{P} \left\{ E_0, R_K^{fs} < R_F \right\} + \mathbb{P} \left\{ E_K, R_K^{ss} < R_F \right\} + \sum_{k=1}^{K-1} \mathbb{P} \left\{ E_k, R_k^{ss} < R_F, R_K^{fs} < R_F \right\}. \quad (9)$$

In (9), the first term calculates the outage probability of the admitted GF user (namely, the  $K$ -th user whose signal is decoded at the first stage of SIC) when all GF users' effective

received powers are larger than  $U_B$ 's decoding threshold  $\tau_0$ ; the second term computes the outage probability of the admitted GF user (the  $K$ -th user whose signal is decoded at the second stage of SIC) when all the users' effective received powers are lower than  $\tau_0$ ; and the third term considers the cases when there are  $k$  ( $1 \leq k \leq K-1$ ) users with effective received powers lower than  $\tau_0$ , the probability of the admitted GF user (either the  $k$ -th user whose signal is decoded at the second stage of SIC, or the  $K$ -th user whose signal is decoded at the first stage of SIC) is in outage.

Note that, in the case of  $|g|^2 < \alpha_B = \frac{\gamma_B}{P_B}$ , the decoding threshold  $\tau_0 \triangleq \max \{0, \alpha_B^{-1}|g|^2 - 1\} = 0$ . Then the outage probability can be expressed as

$$\begin{aligned} \mathcal{P}_{BU} = & \underbrace{\mathbb{P} \{ |g|^2 > \alpha_B, E_0, R_K^{\text{fs}} < R_F \}}_{T_0} + \sum_{k=1}^{K-1} \underbrace{\mathbb{P} \{ |g|^2 > \alpha_B, E_k, R_k^{\text{ss}} < R_F, R_K^{\text{fs}} < R_F \}}_{T_k} \\ & + \underbrace{\mathbb{P} \{ |g|^2 > \alpha_B, E_K, R_K^{\text{ss}} < R_F \}}_{T_K} + \underbrace{\mathbb{P} \{ |g|^2 < \alpha_B, R_K^{\text{fs}} < R_F \}}_{T_{K+1}}, \end{aligned} \quad (10)$$

where the terms  $T_0$ ,  $T_k$  ( $1 \leq k \leq K-1$ ), and  $T_K$  denote the case  $\tau_0 > 0$ . Term  $T_{K+1}$  represents the case  $\tau_0 = 0$ , thus all the GF users' signals should be decoded at the first stage of SIC and  $U_K$  can achieve the maximal data rate in this case. An exact expression of  $\mathcal{P}_{BU}$  is shown in the following theorem.

**Theorem 1.** Assume  $K \geq 2$ . The outage probability of  $U_F$  for BU-SGF scheme,  $\mathcal{P}_{BU}$ , can be approximated as

$$\mathcal{P}_{BU} \approx \begin{cases} \sum_{k=0}^K \bar{\eta}_k G_{1;k} + \sum_{k=0}^K \bar{\eta}_k G_{2;k} + G_3 + I_4, & \text{if } \gamma_B \gamma_F < 1 \\ \sum_{k=0}^K \bar{\eta}_k G_{1;k} + \sum_{k=0}^K \bar{\eta}_k H_{2;k} + G_3, & \text{if } \gamma_B \gamma_F \geq 1 \end{cases}. \quad (11)$$

Here,

$$\begin{aligned} G_{1;k} = & \frac{\alpha_1 - \alpha_B}{2} \sum_{i=1}^I W_i \sqrt{1 - \theta_i^2} f_B(b_i) \left[ F_F \left( \frac{\alpha_B^{-1} b_i - 1}{P_F} \right) \right]^k \\ & \times \left[ F_F(\alpha_F P_B b_i + \alpha_F) - F_F \left( \frac{\alpha_B^{-1} b_i - 1}{P_F} \right) \right]^{K-k}, \end{aligned} \quad (12)$$

$$\begin{aligned} G_{2;k} = & \frac{\alpha_2 - \alpha_1}{2} \sum_{j=1}^J W_j \sqrt{1 - \vartheta_j^2} f_B(d_j) [F_F(\alpha_F)]^k \\ & \times \left[ F_F(\alpha_F P_B d_j + \alpha_F) - F_F \left( \frac{\alpha_B^{-1} d_j - 1}{P_F} \right) \right]^{K-k}, \end{aligned} \quad (13)$$

$$G_3 = \frac{\alpha_B}{2} \sum_{m=1}^M W_m \sqrt{1 - \epsilon_m^2} f_B(e_m) [F_F(\alpha_F P_B e_m + \alpha_F)]^K, \quad (14)$$

$$I_4 = [1 - F_B(\alpha_2)] [F_F(\alpha_F)]^K, \quad (15)$$

$$\begin{aligned} H_{2;k} = & \left( -\frac{1}{2} \right)^{K-k} \frac{[F_F(\alpha_F)]^k}{D_0 + D_1} \sum_{n=1}^N \Phi_n c_n \sum_{m=0}^{K-k} \binom{K-k}{m} (-1)^m \\ & \times \sum_{\sum_{l=0}^L p_l = K-k-m} \binom{K-k-m}{p_0, \dots, p_L} \sum_{\sum_{l=0}^L q_l = m} \binom{m}{q_0, \dots, q_L} \left( \prod_{l=0}^L \Psi_l^{p_l+q_l} \right) \\ & \times e^{\sum_{l=0}^L (q_l \mu_l P_F^{-1} - p_l \mu_l \alpha_F)} \frac{e^{-[\sum_{l=0}^L (p_l \mu_l \alpha_F P_B + q_l \mu_l P_F^{-1} \alpha_B^{-1}) + c_n] \alpha_1}}{\sum_{l=0}^L (p_l \mu_l \alpha_F P_B + q_l \mu_l P_F^{-1} \alpha_B^{-1}) + c_n}, \end{aligned} \quad (16)$$

$W_i = \pi/I$ ,  $\theta_i = \cos[(2i-1)\pi/(2I)]$ ,  $b_i = [(\alpha_1 - \alpha_B)\theta_i + (\alpha_1 + \alpha_B)]/2$ ,  $W_j = \pi/J$ ,  $\vartheta_j = \cos[(2j-1)\pi/(2J)]$ ,  $d_j = [(\alpha_2 - \alpha_1)\vartheta_j + (\alpha_2 + \alpha_1)]/2$ ,  $W_m = \pi/M$ ,  $\epsilon_m = \cos[(2m-1)\pi/(2M)]$ ,  $e_m = (\epsilon_m + 1)\alpha_B/2$ ,  $\bar{\eta}_k = \frac{K!}{k!(K-k)!}$ ,  $\alpha_1 = \alpha_B(\gamma_F + 1)$  and  $\alpha_2 = \frac{\alpha_B(\gamma_F + 1)}{1 - \gamma_B \gamma_F}$ .  $I$ ,  $J$ , and  $M$  are parameters for ensuring complexity-accuracy tradeoff.  $F_F(x)$ ,  $F_B(y)$ , and  $f_B(y)$  are shown in (2), (3), and (4), respectively.

*Proof:* Please refer to Appendix A. ■

*Remark 1:* Following the similar steps for proofing Theorem 1, the outage probability of the BU-SGF scheme in the case of only one GF user, namely,  $K = 1$ , can be derived straightforwardly. We omit it for space limitation.

Since the outage probability  $\mathcal{P}_{BU}$  as derived in Theorem 1 is quite involved, to get some insights, we derive the high SNR approximation and the achieved diversity orders.

**Corollary 1.** Assume  $K \geq 2$  and  $P_B = P_F \rightarrow \infty$ . The high SNR approximation of  $\mathcal{P}_{BU}$  (denoted as  $\vec{\mathcal{P}}_{BU}$ ) can be expressed as

$$\vec{\mathcal{P}}_{BU} = \begin{cases} \sum_{k=0}^K \bar{\eta}_k \vec{I}_{1;k} + \sum_{k=0}^K \bar{\eta}_k \vec{I}_{2;k} + \vec{I}_3 + \vec{I}_4, & \text{if } \gamma_B \gamma_F < 1 \\ \sum_{k=0}^K \bar{\eta}_k \vec{I}_{1;k} + \sum_{k=0}^K \bar{\eta}_k \vec{H}_{2;k} + \vec{I}_3, & \text{if } \gamma_B \gamma_F \geq 1 \end{cases}. \quad (17)$$

Here,

$$\begin{aligned} \vec{I}_{1;k} = & \frac{S_B S_F^K}{P_B^{K+1}} \sum_{i=0}^{K-k} \binom{K-k}{i} (\gamma_F + 1)^{K-k-i} (\gamma_F - \gamma_B^{-1})^i \\ & \times \gamma_B^{i+1} \sum_{j=0}^k \binom{k}{j} (-1)^j \frac{(1 + \gamma_F)^{k-j+i+1} - 1}{k - j + i + 1}, \end{aligned} \quad (18)$$

$$\vec{I}_{2;k} = \frac{S_B S_F^K}{P_B^{K+1}} \sum_{i=0}^{K-k} \binom{K-k}{i} (\gamma_F + 1)^{K-k-i} (\gamma_F - \gamma_B^{-1})^i \gamma_F^k \frac{\tilde{\alpha}_2^{i+1} - \tilde{\alpha}_1^{i+1}}{i+1}, \quad (19)$$

$$\vec{I}_3 = \frac{S_B S_F^K \gamma_F^K}{P_B^{K+1} (K+1)} [(1 + \gamma_B)^{K+1} - 1], \quad (20)$$

$$\vec{I}_4 = \left( \frac{S_F \gamma_F}{P_B} \right)^K \left( 1 - \frac{S_B \tilde{\alpha}_2}{P_B} \right), \quad (21)$$

$$\begin{aligned} \vec{H}_{2;k} = & \left( -\frac{1}{2} \right)^{K-k} \frac{(S_F \gamma_F)^k}{(D_0 + D_1) P_B^k} \sum_{n=1}^N \Phi_n c_n \sum_{m=0}^{K-k} \binom{K-k}{m} \sum_{\sum_{l=0}^L p_l = K-k-m} \binom{K-k-m}{p_0, \dots, p_L} \\ & \times \sum_{\sum_{l=0}^L q_l = m} \binom{m}{q_0, \dots, q_L} \left( \prod_{l=0}^L \Psi_l^{p_l+q_l} \right) \frac{(-1)^m}{\sum_{l=0}^L (p_l \mu_l \gamma_F + q_l \mu_l \gamma_B^{-1}) + c_n}, \end{aligned} \quad (22)$$

$$S_F = \frac{1}{2} \sum_{l=1}^L \Psi_l \mu_l, \quad S_B = \frac{1}{D_0 + D_1} \sum_{n=1}^N \Phi_n c_n, \quad \tilde{\alpha}_1 = \gamma_B (\gamma_F + 1) \text{ and } \tilde{\alpha}_2 = \frac{\gamma_B (\gamma_F + 1)}{1 - \gamma_B \gamma_F}.$$

*Proof:* Please refer to Appendix B. ■

Comparing the terms in (17), we have the following observations. In the case of  $\gamma_B \gamma_F < 1$ ,  $\vec{I}_4$  is inversely proportional to  $P_B^K$ , and all other terms are inversely proportional to  $P_B^{K+1}$ . Furthermore, in the case of  $\gamma_B \gamma_F \geq 1$ ,  $\vec{H}_{2;0}$  is a constant, which is irrelevant to  $P_B$ . Based on the definition of diversity order, namely,  $d = -\lim_{P_B \rightarrow \infty} \frac{\log \vec{P}_{BU}}{\log P_B}$ , we have the following corollary.

**Corollary 2.** Assume  $K \geq 2$  and  $P_B = P_F \rightarrow \infty$ . If  $\gamma_B \gamma_F < 1$ ,  $\vec{P}_{BU}$  can be approximated as  $\left( \frac{S_F \gamma_F}{P_B} \right)^K$ , and  $U_F$  can achieve a diversity order of  $K$ . On the other hand, if  $\gamma_B \gamma_F \geq 1$ ,  $\vec{P}_{BU}$  can be approximated as  $\vec{H}_{2;0}$ , and  $U_F$  can achieve a diversity order of 0.

### B. Performance Analysis for CS-SGF Scheme

Recall that for the CS-SGF scheme, the GF user with the maximal CDF value will be admitted, whose instantaneous channel gain is denoted as  $|h|^2$ . Based on the descriptions in Sections II and III, the outage probability of  $U_F$  can be expressed as

$$\begin{aligned} \mathcal{P}_{CS} = & \underbrace{\mathbb{P} \left\{ |g|^2 < \alpha_B, \frac{P_F |h|^2}{P_B |g|^2 + 1} < \gamma_F \right\}}_{\Delta_1} \\ & + \underbrace{\mathbb{P} \left\{ |g|^2 > \alpha_B, P_F |h|^2 > \tau(|g|^2), \frac{P_F |h|^2}{P_B |g|^2 + 1} < \gamma_F \right\}}_{\Delta_2} \\ & + \underbrace{\mathbb{P} \left\{ |g|^2 > \alpha_B, P_F |h|^2 < \tau(|g|^2), P_F |h|^2 < \gamma_F \right\}}_{\Delta_3}, \end{aligned} \quad (23)$$

where  $\Delta_1$  denotes the case  $\tau_0 = 0$ , and  $U_F$ 's signal is decoded at the first stage of SIC.  $\Delta_2$  ( $\Delta_3$ ) denotes the case when  $\tau_0 > 0$ , and  $U_F$ 's signal is decoded at the first (second) stage of SIC.

**Theorem 2.** The outage probability of  $U_F$  for CS-SGF scheme,  $\mathcal{P}_{CS}$ , can be approximated as

$$\mathcal{P}_{CS} \approx \begin{cases} \frac{\Xi_1 c_n}{\Theta_1} e^{-k\mu_l \alpha_F} (1 - e^{-\Theta_1 \alpha_2}) + \frac{\Xi_1 c_n}{\Theta_2} e^{\frac{k\mu_l}{P_F}} (e^{-\Theta_2 \alpha_2} - e^{-\Theta_2 \alpha_1}) \\ + \Xi_2 e^{-c_n \alpha_1} (1 - e^{-\mu_l \alpha_F})^K, & \text{if } \gamma_B \gamma_F < 1 \\ \frac{\Xi_1 c_n}{\Theta_1} e^{-k\mu_l \alpha_F} - \frac{\Xi_1 c_n}{\Theta_2} e^{\frac{k\mu_l}{P_F}} e^{-\Theta_2 \alpha_1} + \Xi_2 e^{-c_n \alpha_1} (1 - e^{-\mu_l \alpha_F})^K, & \text{if } \gamma_B \gamma_F \geq 1 \end{cases} \quad (24)$$

where  $\Xi_1 = \frac{1}{2(D_1+D_0)} \sum_{l=1}^L \Psi_l \sum_{k=0}^K \binom{K}{k} (-1)^k \sum_{n=1}^N \Phi_n$ ,  $\Xi_2 = \frac{1}{2(D_1+D_0)} \sum_{l=1}^L \Psi_l \sum_{n=1}^N \Phi_n$ ,  $\Theta_1 = k\mu_l P_B \alpha_F + c_n$ , and  $\Theta_2 = \frac{k\mu_l}{P_F \alpha_B} + c_n$ .

*Proof:* Please refer to Appendix C. ■

To obtain more insights, we derive the high SNR asymptotic expressions of the outage probabilities as well.

**Corollary 3.** When  $P_B = P_F \rightarrow \infty$ , if  $\gamma_B \gamma_F < 1$ , the high SNR approximation of  $\mathcal{P}_{CS}$  can be expressed as

$$\begin{aligned} \vec{\mathcal{P}}_{CS} = & \frac{\Xi_2 c_n}{P_B} \left( \frac{\mu_l \gamma_F}{P_B} \right)^K \sum_{k=0}^K \binom{K}{k} \frac{\tilde{\alpha}_2^{k+1}}{k+1} + \Xi_2 \left( \frac{\mu_l \gamma_F}{P_B} \right)^K \\ & + \frac{\Xi_2 c_n \mu_l^K}{P_B^{K+1}} \sum_{k=0}^K \binom{K}{k} (-1)^{K-k} \frac{\tilde{\alpha}_1^{k+1} - \tilde{\alpha}_2^{k+1}}{\gamma_B^k (k+1)}. \end{aligned} \quad (25)$$

If  $\gamma_B \gamma_F \geq 1$ , the high SNR approximation of  $\mathcal{P}_{CS}$  equals

$$\begin{aligned} \vec{\mathcal{P}}_{CS} = & \Xi_1 c_n (\Theta_1^{-1} - \Theta_2^{-1}) + \frac{\Xi_2 c_n \mu_l^K}{P_B^{K+1}} \sum_{k=0}^K \binom{K}{k} (-1)^{K-k} \frac{\gamma_B (1 + \gamma_F)^{k+1} - \gamma_B}{k+1} \\ & + \frac{\Xi_2 c_n}{P_B} \left( \frac{\mu_l \gamma_F}{P_B} \right)^K \sum_{k=0}^K \binom{K}{k} \frac{\gamma_B^{k+1}}{k+1} + \Xi_2 \left( \frac{\mu_l \gamma_F}{P_B} \right)^K. \end{aligned} \quad (26)$$

*Proof:* The high SNR approximation of  $\mathcal{P}_{CS}$  is derived based on (A.37), (A.41), (A.44), and (A.45). When  $P_B = P_F \rightarrow \infty$ , we have  $\alpha_B \rightarrow 0$  and  $\alpha_2 \rightarrow 0$ . By applying  $e^{-x} \approx 1 - x$  for  $x \rightarrow 0$  to (A.37), the high SNR approximation of  $\Delta_1$  can be expressed as

$$\Delta_1 \approx \Xi_2 c_n \mu_l^K \alpha_F^K \int_0^{\alpha_B} (P_B x + 1)^K dx. \quad (27)$$

By applying binomial theorem, (27) can be further derived as

$$\begin{aligned} \Delta_1 \approx & \Xi_2 c_n \mu_l^K \alpha_F^K \int_0^{\alpha_B} \sum_{k=0}^K \binom{K}{k} P_B^k x^k dx \\ \approx & \frac{\Xi_2 c_n}{P_B} \left( \frac{\mu_l \gamma_F}{P_B} \right)^K \sum_{k=0}^K \binom{K}{k} \frac{\gamma_B^{k+1}}{k+1}. \end{aligned} \quad (28)$$

Using (A.41), the high SNR approximation of  $\Delta_2$  in the case of  $\gamma_B\gamma_F < 1$  can be derived as

$$\begin{aligned}\Delta_2 &\approx \Xi_2 c_n \int_{\alpha_B}^{\alpha_2} \left(1 - e^{-\frac{\mu_l \gamma_F (P_B y + 1)}{P_F}}\right)^K dy - \Xi_2 c_n \int_{\alpha_B}^{\alpha_2} \left(1 - e^{-\frac{\mu_l (P_B y - \gamma_B)}{P_F \gamma_B}}\right)^K dy \\ &= \frac{\Xi_2 c_n \mu_l^K \gamma_F^K}{P_B^{k+1}} \sum_{k=0}^K \binom{K}{k} \frac{\tilde{\alpha}_2^{k+1} - \gamma_B^{k+1}}{k+1} - \frac{\Xi_2 c_n \mu_l^K}{P_B^{K+1}} \sum_{k=0}^K \binom{K}{k} (-1)^{K-k} \frac{\tilde{\alpha}_2^{k+1} - \gamma_B^{k+1}}{\gamma_B^k (k+1)}.\end{aligned}\quad (29)$$

By applying (A.44), the high SNR approximation of  $\Delta_2$  in the case of  $\gamma_B\gamma_F \geq 1$  can be expressed as

$$\Delta_2 \approx \Xi_1 c_n (\Theta_1^{-1} - \Theta_2^{-1}). \quad (30)$$

Using (A.45) and following the same lines to derive (28), we can obtain the approximation of  $\Delta_3$  as

$$\Delta_3 \approx \frac{\Xi_2 c_n \mu_l^K}{P_B^{K+1}} \sum_{k=0}^K \binom{K}{k} (-1)^{K-k} \gamma_B \frac{(1 + \gamma_F)^{k+1} - 1}{k+1} + \Xi_2 \left(\frac{\mu_l \gamma_F}{P_B}\right)^K. \quad (31)$$

Finally, we can obtain (25) by combining (28), (29), and (31). Similarly, we can derive (26) by combining (28), (30), and (31). The proof is complete.  $\blacksquare$

We can observe that, the second term of (25) is inversely proportional to  $P_B^K$ , and the other two terms of (25) are inversely proportional to  $P_B^{K+1}$ . Moreover, we can also observe that the first term of (26) is a constant. Hence, we have the following corollary.

**Corollary 4.** When  $P_B = P_F \rightarrow \infty$ , if  $\gamma_B\gamma_F < 1$ ,  $\mathcal{P}_{CS}$  can be further approximated as  $\Xi_2 \left(\frac{\mu_l \gamma_F}{P_B}\right)^K$ , and  $U_F$  can achieve a diversity order of  $K$ . If  $\gamma_B\gamma_F \geq 1$ ,  $\mathcal{P}_{CS}$  can be further approximated as  $\Xi_1 c_n (\Theta_1^{-1} - \Theta_2^{-1})$ , and  $U_F$  can achieve a diversity order of 0.

*Remark 2:* We can see from Corollaries 1 and 4 that, with fixed transmit power, both BU-SGF and CS-SGF schemes can effectively avoid outage error floors and realize robust transmissions only when  $\gamma_B\gamma_F < 1$ . If  $\gamma_B\gamma_F \geq 1$  outage error floors still exist. Similar observation can also be found in [36]. Therefore, in the following, we propose a power control strategy, which can effectively avoid outage error floors in all cases.

## V. POWER CONTROL STRATEGY AND ASSOCIATED PERFORMANCE ANALYSIS

In this section, we first propose a power control strategy to enhance the outage performance by avoiding outage error floors. Then, we will analyze the outage performances of both BU-SGF and CS-SGF schemes after applying the power control strategy.

### A. Proposed Power Control Strategy

Recall that, in both BU-SGF and CS-SGF schemes, the GF users always transmit with fixed power  $P_F$ . If  $U_k$ 's effective received power  $P_F|h_k|^2$  is larger than  $U_B$ 's decoding threshold  $\tau_0$ ,  $U_k$ 's signal should be decoded at the first stage of SIC with a data rate  $\log\left(1 + \frac{P_F|h_k|^2}{P_B|g|^2+1}\right)$ . On the other hand, if  $P_F|h_k|^2 \leq \tau_0$ ,  $U_k$ 's signal will be decoded at the second stage of SIC, with a data rate  $\log(1 + P_F|h_k|^2)$ . We can find that, in the context of  $P_F|h_k|^2 > \tau_0$  and  $\tau_0 > 0$ ,  $U_k$  can reduce its transmit power  $P_F$  less than  $\frac{\tau_0}{|h_k|^2}$  to make its signal be decoded at the second stage of SIC, and the achievable rate will be changed from  $\log\left(1 + \frac{P_F|h_k|^2}{P_B|g|^2+1}\right)$  to  $\log(1 + P'_F|h_k|^2)$  accordingly, where  $P'_F \leq \frac{\tau_0}{|h_k|^2}$ . On the other hand, if  $P_F|h_k|^2 < \tau_0$  and  $P_m|h_k|^2 > \tau_0$ ,  $U_k$  can increase its transmit power and transform its rate from  $\log(1 + P_F|h_k|^2)$  to  $\log\left(1 + \frac{P''_F|h_k|^2}{P_B|g|^2+1}\right)$ , where  $\frac{\tau_0}{|h_k|^2} < P''_F \leq P_m$ . This is the motivation of our power control strategy.

The goal of our power control strategy is to maximize each GF user's data rate. Here,  $P_k$  should be set as  $P_m$ , since both  $\log\left(1 + \frac{P_k|h_k|^2}{P_B|g|^2+1}\right)$  and  $\log(1 + P_k|h_k|^2)$  are mono-increasing functions of  $P_k$ . But when  $U_k$ 's maximal effective received power is larger than  $U_B$ 's decoding threshold, namely,  $P_m|h_k|^2 > \tau_0$ ,  $U_k$  may tune its transmit power based on the values of  $\log\left(1 + \frac{P_m|h_k|^2}{P_B|h_B|^2+1}\right)$  (namely, decoding its signal at the first stage of SIC) and  $\log(1 + \tau_0)$  (namely, decoding its signal at the second stage of SIC). To be specific, in the case of  $P_m|h_k|^2 > \tau_0$ ,  $P_k$ 's transmit power may be set as  $P_m$  or  $\frac{\tau_0}{|h_k|^2}$  in order to maximize  $U_k$ 's data rate, and the achievable rate is  $\log\left(1 + \frac{P_m|h_k|^2}{P_B|h_B|^2+1}\right)$  or  $\log(1 + \tau_0)$ , respectively. Hence, the power control strategy for  $U_k$  is

$$P_k = \begin{cases} \frac{\tau_0}{|h_k|^2}, & \text{if } \frac{\tau_0}{P_m} < |h_k|^2 < \frac{\tau_0(1+P_B|g|^2)}{P_m} \\ P_m, & \text{otherwise} \end{cases}. \quad (32)$$

*Remark 3:* Compared to fixed transmit power strategy in BU-SGF and CS-SGF schemes, the proposed power control strategy does not introduce extra signaling overhead and can be executed distributedly. We can see from (32) that  $P_k$  is decided by  $U_k$ 's maximal transmit power  $P_m$ ,  $|h_k|^2$ ,  $\tau_0$ , and  $P_B|g|^2$ . Note that,  $P_m$  and  $|h_k|^2$  are already known by  $U_k$ , while  $\tau_0$  and  $P_B|g|^2$  are also needed to be broadcasted by the BS for BU-SGF and CS-SGF schemes.

In the following, the outage probabilities and the achieved diversity orders will be derived for both BU-SGF scheme applied with power control strategy (BU-SGF-PC) and CS-SGF scheme applied with power control strategy (CS-SGF-PC).

### B. Performance Analysis for BU-SGF-PC Scheme

Following the same steps of deriving (10), the admitted GF user's outage probability for BU-SGF-PC scheme can be calculated as

$$\begin{aligned}
\mathcal{P}_{BU}^{\text{PC}} = & \underbrace{\mathbb{P} \left\{ |g|^2 > \alpha_B, E_0^{\text{PC}}, \gamma_K^{\text{fs}} > \tau(|g|^2), \gamma_K^{\text{fs}} < \gamma_F \right\}}_{T_{0,1}^{\text{PC}}} \\
& + \underbrace{\mathbb{P} \left\{ |g|^2 > \alpha_B, E_0^{\text{PC}}, \gamma_K^{\text{fs}} < \tau(|g|^2), \tau(|g|^2) < \gamma_F \right\}}_{T_{0,2}^{\text{PC}}} \\
& + \sum_{k=1}^{K-1} \underbrace{\mathbb{P} \left\{ |g|^2 > \alpha_B, E_k^{\text{PC}}, \gamma_k^{\text{ss}} < \gamma_F, \gamma_K^{\text{fs}} > \tau(|g|^2), \gamma_K^{\text{fs}} < \gamma_F \right\}}_{T_{k,1}^{\text{PC}}} \\
& + \sum_{k=1}^{K-1} \underbrace{\mathbb{P} \left\{ |g|^2 > \alpha_B, E_k^{\text{PC}}, \gamma_k^{\text{ss}} < \gamma_F, \gamma_K^{\text{fs}} < \tau(|g|^2), \tau(|g|^2) < \gamma_F \right\}}_{T_{k,2}^{\text{PC}}} \\
& + \underbrace{\mathbb{P} \left\{ |g|^2 > \alpha_B, E_K^{\text{PC}}, \gamma_K^{\text{ss}} < \gamma_F \right\}}_{T_K^{\text{PC}}} + \underbrace{\mathbb{P} \left\{ |g|^2 < \alpha_B, \gamma_K^{\text{fs}} < \gamma_F \right\}}_{T_{K+1}^{\text{PC}}},
\end{aligned} \tag{33}$$

where  $\gamma_k^{\text{fs}} = \frac{P_m |h_k|^2}{P_B |g|^2 + 1}$  and  $\gamma_k^{\text{ss}} = P_m |h_k|^2$ .  $E_k^{\text{PC}}$  ( $1 \leq k \leq K$ ) denotes the event that there are  $k$  users' maximal received powers are less than  $\tau_0$ .  $T_{K+1}^{\text{PC}}$  denotes the outage probability of the admitted GF user  $U_K$  when  $\tau_0 = 0$ , while the other terms represent the case  $\tau_0 > 0$ . More specifically,  $T_0^{\text{PC}} \triangleq T_{0,1}^{\text{PC}} + T_{0,2}^{\text{PC}}$  denotes, when all GF users' maximal effective received powers are above  $\tau_0$ , the outage probability of the admitted GF user  $U_K$ , whose signal is transmitted with power  $P_m$  if  $\gamma_K^{\text{fs}} > \tau(|g|^2)$ , or with power  $\frac{\tau(|g|^2)}{|h_K|^2}$  if  $\gamma_K^{\text{fs}} < \tau(|g|^2)$ . Similarly,  $T_k^{\text{PC}} \triangleq T_{k,1}^{\text{PC}} + T_{k,2}^{\text{PC}}$  represents, when there are  $k$  ( $1 \leq k \leq K-1$ ) users' maximal effective received powers are above  $\tau_0$ , the outage probability of the admitted GF user ( $U_k$  or  $U_K$ ). Here,  $U_K$ 's signal is transmitted with power  $P_m$  if  $\gamma_K^{\text{fs}} > \tau(|g|^2)$ , or with power  $\frac{\tau(|g|^2)}{|h_K|^2}$  if  $\gamma_K^{\text{fs}} < \tau(|g|^2)$ .  $T_K^{\text{PC}}$  shows, when all the  $K$  GF users maximal effective received powers are less than  $\tau_0$ , the outage probability of the admitted GF user ( $U_K$  in this case).

**Theorem 3.** *The outage probability of  $U_F$  for BU-SGF-PC scheme,  $\mathcal{P}_{BU}^{\text{PC}}$ , can be expressed as*

$$\mathcal{P}_{BU}^{\text{PC}} \approx \sum_{k=0}^K \bar{\eta}_k G_{1;k}(P_F \mapsto P_m) + G_3(P_F \mapsto P_m) + I_5, \tag{34}$$

where

$$I_5 = [1 - F_B(\alpha_1)] \left[ F_F \left( \frac{\gamma_F}{P_m} \right) \right]^K. \tag{35}$$

*Proof:* Please refer to Appendix D. ■

**Corollary 5.** When  $P_B = P_m \rightarrow \infty$ , the high SNR approximation of  $\mathcal{P}_{BU}^{PC}$  can be expressed as

$$\vec{\mathcal{P}}_{BU}^{PC} = \sum_{k=0}^K \bar{\eta}_k \vec{I}_{1;k} + \vec{I}_3 + \left( \frac{S_F \gamma_F}{P_B} \right)^K \left( 1 - \frac{S_B \tilde{\alpha}_1}{P_B} \right). \quad (36)$$

*Proof:* Equation (36) can be derived by following the same steps of deriving (17), and we omit here for space limitation. ■

Similar with the derivation of Corollary 2, we have the following corollary.

**Corollary 6.** When  $P_B = P_m \rightarrow \infty$ ,  $\mathcal{P}_{BU}^{PC}$  can be further approximated as  $\left( \frac{S_F \gamma_F}{P_B} \right)^K$ , and  $U_F$  can achieve a diversity order of  $K$ .

### C. Performance Analysis for CS-SGF-PC Scheme

Similar with (23), the outage probability of  $U_F$  for CS-SGF-PC scheme can be formulated as

$$\begin{aligned} \mathcal{P}_{CS}^{PC} = & \underbrace{\mathbb{P}\{|g|^2 < \alpha_B, \frac{P_m|h|^2}{P_B|g|^2 + 1} < \gamma_F\}}_{\Delta_1} + \underbrace{\mathbb{P}\{|g|^2 > \alpha_B, P_m|h|^2 < \tau(|g|^2), P_m|h|^2 < \gamma_F\}}_{\Delta_3} \\ & + \underbrace{\mathbb{P}\{|g|^2 > \alpha_B, P_m|h|^2 > \tau(|g|^2), \frac{P_m|h|^2}{P_B|g|^2 + 1} > \tau(|g|^2), \frac{P_m|h|^2}{P_B|g|^2 + 1} < \gamma_F\}}_{\Delta_4} \\ & + \underbrace{\mathbb{P}\{|g|^2 > \alpha_B, P_m|h|^2 > \tau(|g|^2), \frac{P_m|h|^2}{P_B|g|^2 + 1} < \tau(|g|^2), \tau(|g|^2) < \gamma_F\}}_{\Delta_5}, \end{aligned} \quad (37)$$

where  $\Delta_4$  and  $\Delta_5$  represent, when  $P_m|h|^2 > \tau(|g|^2)$ ,  $U_F$ 's signal is transmitted with power  $P_m$  and  $\frac{\tau(|g|^2)}{|h|^2}$  (here  $\tau_0 = \tau(|g|^2)$ , since  $|g|^2 > \alpha_B$  in  $\Delta_4$  and  $\Delta_5$ ), respectively.

**Theorem 4.** The outage probability of  $U_F$  for CS-SGF-PC scheme can be approximated as

$$\mathcal{P}_{CS}^{PC} \approx \frac{\Xi_1 c_n}{\Theta_1} e^{-\frac{k \mu_F \gamma_F}{P_m}} \left( 1 - e^{-\Theta_1 \alpha_1} \right) + \Xi_2 e^{-c_n \alpha_1} \left( 1 - e^{-\frac{\mu_F \gamma_F}{P_m}} \right)^K. \quad (38)$$

*Proof:* We simplify (37) first. Note that  $\Delta_4$  and  $\Delta_5$  can be respectively converted to

$$\Delta_4 = \mathbb{P} \left\{ \alpha_B < |g|^2 < \alpha_1, \frac{P_B|g|^2 + 1}{P_m} \tau(|g|^2) < |h|^2 < \frac{P_B|g|^2 + 1}{P_m} \gamma_F \right\} \quad (39)$$

and

$$\Delta_5 = \mathbb{P} \left\{ \alpha_B < |g|^2 < \alpha_1, \frac{\tau(|g|^2)}{P_m} < |h|^2 < \frac{P_B|g|^2 + 1}{P_m} \tau(|g|^2) \right\}. \quad (40)$$

Combining (39) and (40),  $\Delta_4 + \Delta_5$  can be represented as

$$\Delta_4 + \Delta_5 = \mathbb{P} \left\{ \alpha_B < |g|^2 < \alpha_1, \frac{\tau(|g|^2)}{P_m} < |h|^2 < \frac{P_B|g|^2 + 1}{P_m} \gamma_F \right\}. \quad (41)$$

By applying (A.12),  $\Delta_3$  can be rewritten as

$$\Delta_3 = \mathbb{P} \left\{ \alpha_B < |g|^2 < \alpha_1, |h|^2 < \frac{\tau(|g|^2)}{P_m} \right\} + \mathbb{P} \left\{ |g|^2 > \alpha_1, |h|^2 < \frac{\gamma_F}{P_m} \right\}. \quad (42)$$

Then the sum of  $\Delta_3$ ,  $\Delta_4$  and  $\Delta_5$  can be expressed as

$$\begin{aligned} \Delta_3 + \Delta_4 + \Delta_5 &= \mathbb{P} \left\{ \alpha_B < |g|^2 < \alpha_1, |h|^2 < \frac{P_B |g|^2 + 1}{P_m} \gamma_F \right\} \\ &\quad + \mathbb{P} \left\{ |g|^2 > \alpha_1, |h|^2 < \frac{\gamma_F}{P_m} \right\}. \end{aligned} \quad (43)$$

Finally, by combining  $\Delta_1$  and (43),  $\mathcal{P}_{CS}^{PC}$  can be simplified as

$$\mathcal{P}_{CS}^{PC} = \mathbb{P} \left\{ |g|^2 < \alpha_1, |h|^2 < \frac{P_B |g|^2 + 1}{P_m} \gamma_F \right\} + \mathbb{P} \left\{ |g|^2 > \alpha_1, |h|^2 < \frac{\gamma_F}{P_m} \right\}. \quad (44)$$

Following the same steps for the derivation of Theorem 2, we can obtain (38), and the proof is complete.  $\blacksquare$

Next, we derive the high SNR asymptotic expression of the outage probability.

**Corollary 7.** Assuming  $P_B = P_m \rightarrow \infty$ , the high SNR approximation of  $\mathcal{P}_{CS}^{PC}$  equals

$$\vec{\mathcal{P}}_{CS}^{PC} = \frac{\Xi_2 c_n}{P_B} \left( \frac{\mu_l \gamma_F}{P_B} \right)^K \sum_{k=0}^K \binom{K}{k} \frac{(\gamma_B + \gamma_B \gamma_F)^{k+1}}{k+1} + \Xi_2 \left( \frac{\mu_l \gamma_F}{P_B} \right)^K. \quad (45)$$

*Proof:* Equation (45) can be derived by following the similar steps of deriving (25), and we omit here for space limitation.  $\blacksquare$

Similar to Corollary 4, we can obtain the following corollary from (45).

**Corollary 8.** Assuming  $P_B = P_m \rightarrow \infty$ ,  $\mathcal{P}_{CS}^{PC}$  can be further approximated as  $\Xi_2 \left( \frac{\mu_l \gamma_F}{P_B} \right)^K$ , and  $U_F$  can achieve a diversity order of  $K$ .

*Remark 4:* We can observe from Corollaries 4 and 8 that both CS-SGF and CS-SGF-PC schemes have the same high SNR approximation and can achieve the same diversity order in the case of  $\gamma_B \gamma_F < 1$ . Similar observation can be found for BU-SGF and BU-SGF-PC schemes. We will see in the simulation results that CS-SGF-PC (BU-SGF-PC) scheme can achieve much better outage performance than CS-SGF (BU-SGF) scheme at the moderate SNR region.

*Remark 5:* From the derivation process of Theorem 1 and Corollaries 1 and 2 (Theorem 2 and Corollaries 3 and 4), we can see that, for BU-SGF (CS-SGF) scheme and in the case of  $\gamma_B \gamma_F \geq 1$ , the outage error floor results from  $I_{2;k}$  in (A.29) ( $\Delta_2$  in (A.43)). Specifically, the unrestriction of GB's channel gain leads to the outage error floor. However, we can observe from the derivation process of Theorem 3 (Theorem 4) that, an additional constraint of  $|g|^2 < \alpha_1$  is introduced after

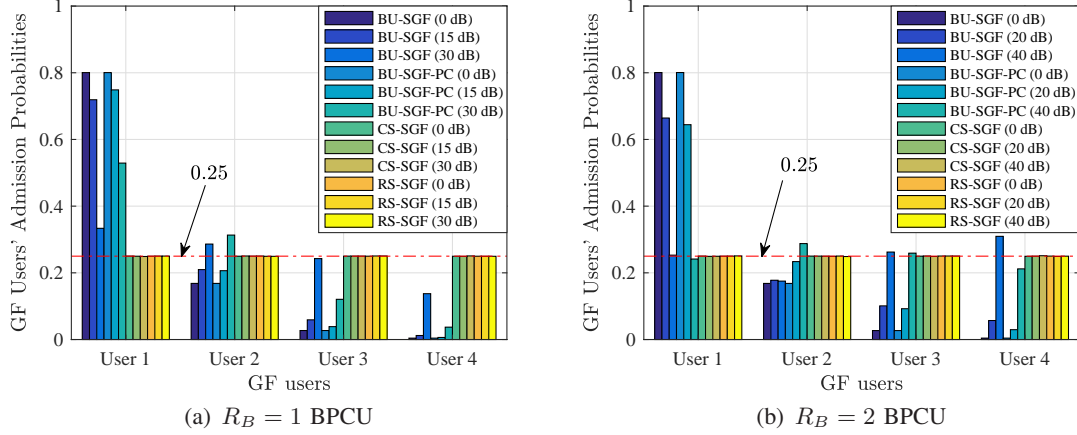


Fig. 1. GF users' admission probabilities comparison of different schemes.

applying the proposed power control strategy, which effectively removes the error floor.

*Remark 6:* Although Theorems 2 and 4 are derived for CS-SGF and CS-SGF-PC schemes, in the spacial case of  $K = 1$ , these expressions can also be used to evaluate the performance of random selection SGF scheme with HSIC decoding (RS-SGF), which can also achieve fair access for the GF users. That is because all the GF users are randomly distributed within  $\mathcal{D}_F$  with the same distribution, and these distributions are independent with each other.

## VI. SIMULATION RESULTS AND DISCUSSIONS

In this section, the accuracy of the theoretical analyses and performance of different SGF transmission schemes are examined through computer simulations, where the GB and GF users are respectively randomly distributed in  $\mathcal{D}_B$  and  $\mathcal{D}_F$  in each trial. In existing studies, only [33], [34] investigated the impact of user locations on SGF schemes. The random selection SGF scheme with fixed SIC orders (termed as RS-SGF-FSIC) proposed in [33], [34] is used as benchmark, where the GF user is randomly selected from all the GF users. Hereinafter, unless other specified, the simulation parameters are set as  $\alpha = 3$ ,  $K = 4$ ,  $D_F = D_1 = 3$  m,  $D_0 = 1$  m,  $R_B = 1$  bits per channel use (BPCU),  $R_F = 0.9$  BPCU,  $P_B = P_m$ , and  $P_F = P_m$  for the schemes without power control (namely, BU-SGF, CS-SGF, and RS-SGF schemes). All the complexity-accuracy tradeoff parameters are set as 10.

Fig. 1 compares GF users' admission probabilities of different schemes in 4-user case, where the distances from the 4 GF users to the BS vary from 1 m to 4 m with an interval of 1 m, and  $U_B$ 's distance is 2 m. We only plot the admission probability of CS-SGF scheme, since CS-SGF-PC and CS-SGF schemes have the same fairness performance. We can see that both CS-SGF

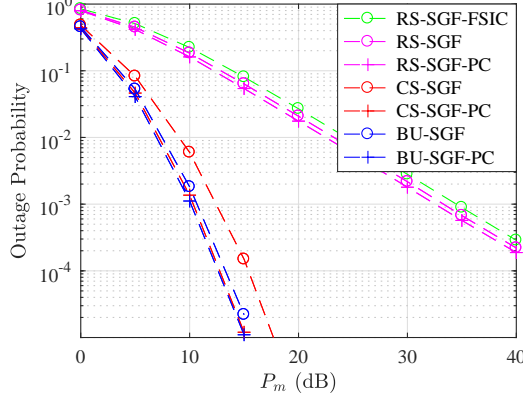


Fig. 2. Outage probability comparison of different SGF schemes, where  $D_F = D_0 = 1$  m,  $D_1 = 3$  m, and  $P_B = 10$  dB.

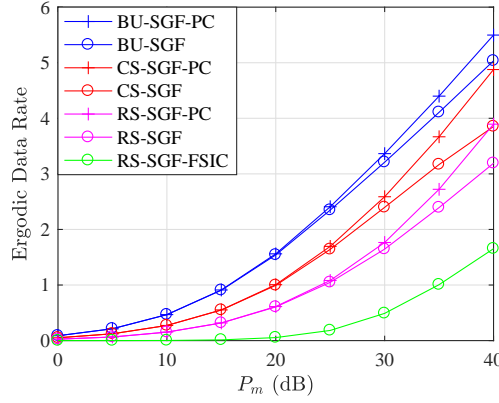


Fig. 3. GF users' ergodic data rate comparison of different SGF schemes, where  $D = D_1 = 10$ ,  $D_0 = 1$  m, and  $R_B = 1$  BPCU.

and RS-SGF schemes can achieve fair admission probability for each GF user. However, for the BU-SGF and BU-SGF-PC schemes, the users closer to the BS become more preferred to be admitted.

The outage probabilities of different SGF schemes are compared in Fig. 2. For ease of comparison with RS-SGF-FSIC scheme [33], we set  $D_F = D_0 = 1$  m,  $D_1 = 3$  m, and  $P_B = 10$  dB. The performance of RS-SGF(-PC) scheme is plotted as well. We can see that, the outage probability of CS-SGF(-PC) scheme is much superior than RS-SGF(-PC) scheme, but inferior to BU-SGF(-PC) schemes for the price of fairness. We can also see that CS-SGF(-PC) and BU-SGF(-PC) schemes can achieve much higher diversity orders than RS-SGF(-PC) and RS-SGF-FSIC schemes due to the higher slope of the outage probability curves at high SNR region.

Fig. 3 depicts the ergodic data rates of different SGF schemes, where  $D_F = D_1 = 10$ ,  $D_0 = 1$  m, and  $R_B = 1$  BPCU for facilitating comparison with RS-SGF-FSIC scheme [34]. It can be observed that all the schemes applying HSIC can achieve better ergodic data rate

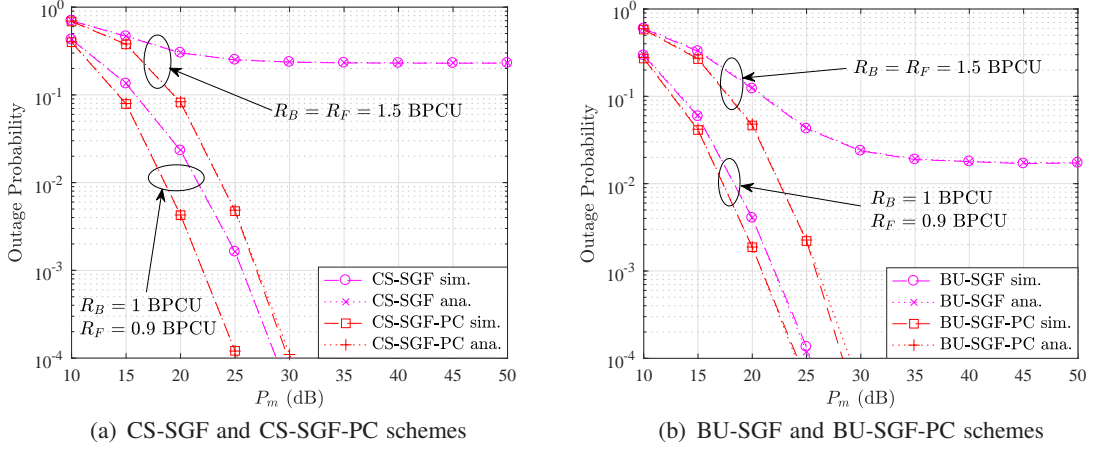


Fig. 4. Accuracy of analytical results, where  $K = 3$ .

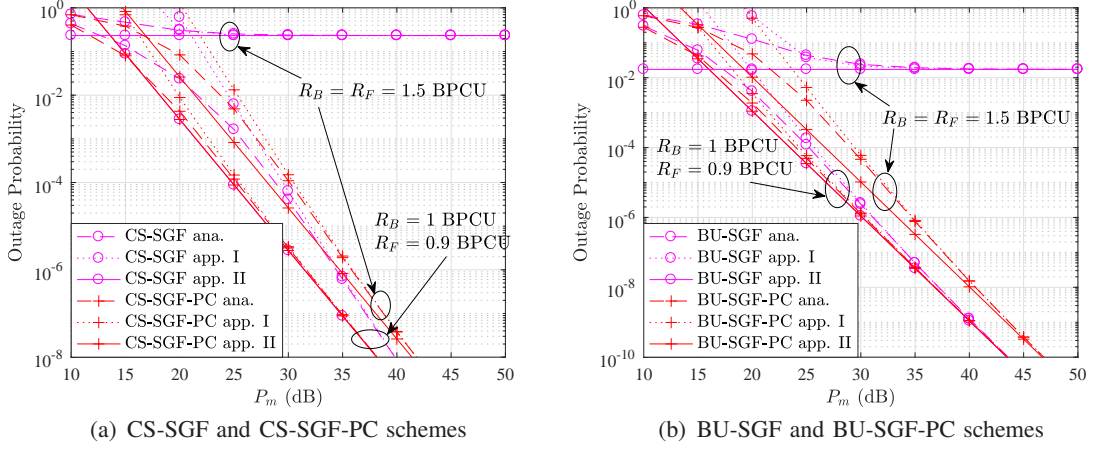


Fig. 5. Accuracy of approximation expressions, where  $K = 3$ .

performance than RS-SGF-FSIC scheme, where such improvement comes from effective use of multiuser diversity and HSIC. It can also be observed that the proposed power control strategy can effectively improve the ergodic data rate. Moreover, we can also observe that the BU-SGF (BU-SGF-PC) scheme can achieve the best performance, while the CS-SGF (CS-SGF-PC) scheme can achieve fair admission probability at the price of inferior data rate.

In Fig. 4, the accuracy of the analytical results is evaluated, which are based on Theorems 1–4. The number of GF users are set as  $K = 3$ . We can see from Fig. 4 that the simulation matches well with the analytical results for both CS-SGF (-PC) and BU-SGF (-PC) schemes, which demonstrates the accuracy of Theorems 1–4. We can also observe from Fig. 4 that the proposed power control scheme can effectively improve the outage performance.

Fig. 5 evaluates the accuracy of the approximations derived in Corollaries 1–8. In the figure,

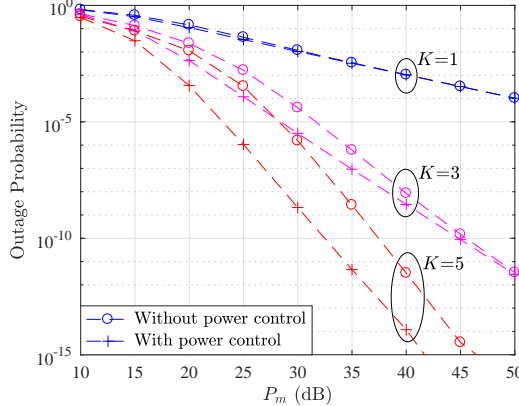


Fig. 6. Outage probability versus SNR with different  $K$ .

curves labeled ‘‘approximation I’’ are depicted based on Corollaries 1, 3, 5, and 7, while these labeled ‘‘approximation II’’ represent the results from Corollaries 2, 4, 6, and 8. It can be observed from the two subfigures that all the high SNR approximations match well with the simulation results in high SNR region. As shown in Corollaries 2 and 4, for both BU-SGF and CS-SGF schemes, zero diversity orders are achieved (namely, outage error floors exist) when the product of two users’ target SINRs are larger than 1, or full diversity orders otherwise. However, as shown in the Fig. 5 and demonstrated in Corollaries 6 and 8 that, BU-SGF-PC and CS-SGF-PC schemes can achieve full diversity orders even if the product of two users’ target SINRs is larger than 1.

The outage probabilities of CS-SGF and CS-SGF-PC schemes versus SNR with different number of GF users are shown in Fig. 6. We also plot the analytical results for RS-SGF and RS-SGF-PC schemes by setting  $K = 1$  according to Remark 6. It can be seen that the outage performance of the two schemes are improved with the increasing number of GF users, which verify that the fair SGF schemes, namely, CS-SGF and CS-SGF-PC schemes, can effectively utilize multiuser diversity. It can also been seen that the proposed power control strategy can improve the outage performance at the moderate SNR region when the product of the two users’ target SINR is less than 1.

Fig. 7 depicts the outage probability versus SNR with different path loss exponents and rate-pairs, where rate-pair denotes the pair of target data rates of the GB and GF users. Three rate-pairs are evaluated, specifically, for rate-pair I,  $R_B=1$  BPCU,  $R_F=0.5$  BPCU; for rate-pair II,  $R_B=1$  BPCU,  $R_F=0.9$  BPCU, and for rate-pair III,  $R_B=1.5$  BPCU,  $R_F=0.9$  BPCU. We can see that the outage probability increases with the increase of GB/GF user’s rate or the path loss exponent.

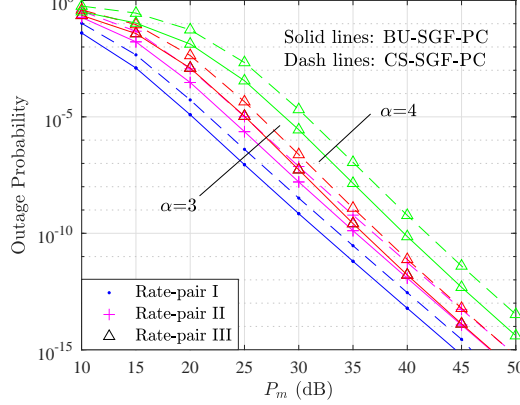


Fig. 7. Outage probability versus SNR with different rate pairs and path loss exponents. For rate-pair I,  $R_B=1$  BPCU,  $R_F=0.5$  BPCU; for rate-pair II,  $R_B=1$  BPCU,  $R_F=0.9$  BPCU; and for rate-pair III,  $R_B=1.5$  BPCU,  $R_F=0.9$  BPCU.

Another interesting observation is that the outage probability of rate-pair II and rate-pair III superimpose at high SNR region for both BU-SGF-PC and CS-SGF-PC schemes. That can be explained by Corollaries 6 and 8, which show that the GF users' high SNR approximations of both BU-SGF-PC and CS-SGF-PC schemes are decided by GB users' power and GF users' target rates.

## VII. CONCLUSIONS

In this paper, we have studied the outage performance of two kinds of NOMA assisted SGF schemes in the system with randomly deployed users, namely, performance oriented SGF scheme and fairness oriented SGF scheme. A distributed power control strategy is invoked to effectively enhance the outage performance and relax the data rate constraint of the admitted users for achieving full diversity orders. Closed-form expressions of the admitted GF users' outage probabilities and achieved diversity orders are derived for both CS-SGF (-PC) and BU-SGF (-PC) schemes. Simulation results verified the analytical results and the effectiveness of the proposed power control strategy.

## APPENDIX A PROOF OF THEOREM 1

### A. Calculation of $T_0$

Recall that  $T_0$  can be expressed as

$$\begin{aligned} T_0 &= \mathbb{P} \left\{ |g|^2 > \alpha_B, P_F |h_1|^2 > \tau(|g|^2), \log \left( 1 + \frac{P_F |h_K|^2}{P_B |g|^2 + 1} \right) < R_F \right\} \\ &= \mathbb{P} \left\{ |g|^2 > \alpha_B, |h_1|^2 > \frac{\tau(|g|^2)}{P_F}, |h_K|^2 < \alpha_F (P_B |g|^2 + 1) \right\}. \end{aligned} \quad (\text{A.1})$$

Note that since  $|h_1|^2$  should be no larger than  $|h_K|^2$ , there is a hidden constraint in (A.1) that  $\frac{\tau(|g|^2)}{P_F}$  should be smaller than  $\alpha_F(P_B|g|^2 + 1)$ . By applying  $\tau(|g|^2) = \alpha_B^{-1}|g|^2 - 1$  and after some algebraic calculations, we have  $\frac{\tau(|g|^2)}{P_F} < \alpha_F(P_B|g|^2 + 1)$  holds under the following two cases

$$\begin{cases} |g|^2 < \alpha_2, & \text{if } \gamma_B \gamma_F < 1 \\ \text{No constraint,} & \text{if } \gamma_B \gamma_F \geq 1 \end{cases}, \quad (\text{A.2})$$

where  $\alpha_2 = \frac{\alpha_B(1+\gamma_F)}{1-\gamma_B\gamma_F}$ . In the following, we will first focus the derivation on the case  $\gamma_B \gamma_F < 1$ , and the case of  $\gamma_B \gamma_F \geq 1$  will be derived at the end of this subsection.

When  $\gamma_B \gamma_F < 1$ , (A.1) can be further rewritten as

$$T_0 = \mathbb{P} \left\{ \alpha_B < |g|^2 < \alpha_2, |h_1|^2 > \frac{\tau(|g|^2)}{P_F}, |h_K|^2 < \alpha_F(P_B|g|^2 + 1) \right\}, \quad (\text{A.3})$$

since  $\alpha_B < \alpha_2$ . Thus,  $T_0$  is related to three random variables  $|g|^2$ ,  $|h_1|^2$ , and  $|h_K|^2$ , where  $|h_1|^2$  and  $|h_K|^2$  are two order statistics, and  $|g|^2$  is independent of them. The joint pdf of  $|h_1|^2$  and  $|h_K|^2$  can be expressed as [45]

$$f_{|h_1|^2, |h_K|^2}(x, y) = \tilde{\eta}_0 f_F(x) f_F(y) [F_F(y) - F_F(x)]^{K-2}, \quad (\text{A.4})$$

where  $x \leq y$  and  $\tilde{\eta}_0 = K(K-1)$ . By applying (A.4),  $T_0$  can be expressed as

$$T_0 = \int_{\alpha_B}^{\alpha_2} f_B(w) \int_{\frac{\alpha_B^{-1}w-1}{P_F}}^{\alpha_F(P_Bw+1)} \int_x^{\alpha_F(P_Bw+1)} \tilde{\eta}_0 f_F(x) f_F(y) [F_F(y) - F_F(x)]^{K-2} dy dx dw. \quad (\text{A.5})$$

We first calculate the following integral:

$$\begin{aligned} & \int_{\frac{\alpha_B^{-1}w-1}{P_F}}^{\alpha_F(P_Bw+1)} \int_x^{\alpha_F(P_Bw+1)} f_F(x) f_F(y) [F_F(y) - F_F(x)]^{K-2} dy dx \\ &= \int_{\frac{\alpha_B^{-1}w-1}{P_F}}^{\alpha_F(P_Bw+1)} \frac{1}{K-1} f_F(x) [F_F(\alpha_F P_B w + \alpha_F) - F_F(x)]^{K-1} dx \\ &= \frac{1}{K(K-1)} \left[ F_F(\alpha_F P_B w + \alpha_F) - F_F \left( \frac{\alpha_B^{-1}w-1}{P_F} \right) \right]^K. \end{aligned} \quad (\text{A.6})$$

By using the result in (A.6) and  $\tau(|g|^2) = \alpha_B^{-1}|g|^2 - 1$ ,  $T_0$  can be finally represented as

$$T_0 = I_{1;0} + I_{2;0}, \quad (\text{A.7})$$

where

$$I_{1;k} = \int_{\alpha_B}^{\alpha_1} f_B(w) \left[ F_F \left( \frac{\alpha_B^{-1}w-1}{P_F} \right) \right]^k \left[ F_F(\alpha_F P_B w + \alpha_F) - F_F \left( \frac{\alpha_B^{-1}w-1}{P_F} \right) \right]^{K-k} dw, \quad (\text{A.8})$$

$$I_{2;k} = \int_{\alpha_1}^{\alpha_2} f_B(w) [F_F(\alpha_F)]^k \left[ F_F(\alpha_F P_B w + \alpha_F) - F_F\left(\frac{\alpha_B^{-1}w - 1}{P_F}\right)\right]^{K-k} dw. \quad (\text{A.9})$$

### B. Calculation of $T_k$ ( $1 \leq k \leq K-1$ )

Recall that  $T_k$  can be expressed as

$$\begin{aligned} T_k &= \mathbb{P} \left\{ |g|^2 > \alpha_B, E_k, \log(1 + P_F |h_k|^2) < R_F, \log\left(1 + \frac{P_F |h_K|^2}{P_B |g|^2 + 1}\right) < R_F \right\} \\ &= \mathbb{P} \left\{ |g|^2 > \alpha_B, |h_k|^2 < \alpha_F, P_F |h_k|^2 < \tau(|g|^2), \right. \\ &\quad \left. P_F |h_{k+1}|^2 > \tau(|g|^2), |h_K|^2 < \alpha_F (P_B |g|^2 + 1) \right\}. \end{aligned} \quad (\text{A.10})$$

Since  $|h_{k+1}|^2$  should be no larger than  $|h_K|^2$ , by applying the hidden constraint in (A.2),  $T_k$  can be rewritten as

$$\begin{aligned} T_k &= \mathbb{P} \left\{ \alpha_B < |g|^2 < \alpha_2, |h_k|^2 < \alpha_F, |h_k|^2 < \frac{\tau(|g|^2)}{P_F}, \right. \\ &\quad \left. |h_{k+1}|^2 > \frac{\tau(|g|^2)}{P_F}, |h_K|^2 < \alpha_F (P_B |g|^2 + 1) \right\}, \end{aligned} \quad (\text{A.11})$$

when  $\gamma_B \gamma_F < 1$ .

In (A.11), one of the constraints of  $|h_k|^2$  can be eliminated based on the value range of  $|g|^2$ .

Note that

$$\begin{cases} \alpha_F < \frac{\tau(|g|^2)}{P_F}, & \text{if } |g|^2 > \alpha_1 \\ \alpha_F \geq \frac{\tau(|g|^2)}{P_F}, & \text{otherwise} \end{cases}, \quad (\text{A.12})$$

where  $\alpha_1 = (1 + \gamma_F) \alpha_B$ , and  $\alpha_B < \alpha_1 < \alpha_2 = \frac{\alpha_B(1 + \gamma_F)}{1 - \gamma_B \gamma_F}$ . Then, by applying (A.12),  $T_k$  equals

$$\begin{aligned} T_k &= \mathbb{P} \left\{ \alpha_B < |g|^2 < \alpha_1, |h_k|^2 < \frac{\tau(|g|^2)}{P_F}, |h_{k+1}|^2 > \frac{\tau(|g|^2)}{P_F}, |h_K|^2 < \alpha_F (P_B |g|^2 + 1) \right\} \\ &\quad + \mathbb{P} \left\{ \alpha_1 < |g|^2 < \alpha_2, |h_k|^2 < \alpha_F, |h_{k+1}|^2 > \frac{\tau(|g|^2)}{P_F}, |h_K|^2 < \alpha_F (P_B |g|^2 + 1) \right\}. \end{aligned} \quad (\text{A.13})$$

We consider the following two cases to calculate  $T_k$ .

1)  $1 \leq k \leq K-2$ : In this case,  $|h_{k+1}|^2$  and  $|h_K|^2$  are two different variables. The joint pdf of  $|h_k|^2$ ,  $|h_{k+1}|^2$ , and  $|h_K|^2$  is [45]

$$f_{|h_k|^2, |h_{k+1}|^2, |h_K|^2}(x, y, z) = \eta_k f_F(x) [F_F(x)]^{k-1} f_F(y) [F_F(z) - F_F(y)]^{K-k-2} f_F(z), \quad (\text{A.14})$$

where  $x \leq y \leq z$ , and  $\eta_k = \frac{K!}{(k-1)!(K-k-2)!}$ .

Since the  $U_B$ 's channel gain  $|g|^2$  is independent with  $|h_k|^2$ ,  $|h_{k+1}|^2$ , and  $|h_K|^2$ , by applying (A.14),  $T_k$  can be expressed as

$$\begin{aligned} T_k = & \int_{\alpha_B}^{\alpha_1} f_B(w) \int_0^{\frac{\alpha_B^{-1}w-1}{P_F}} \eta_k f_F(x) [F_F(x)]^{k-1} \int_{\frac{\alpha_B^{-1}w-1}{P_F}}^{\alpha_F(P_Bw+1)} \int_y^{\alpha_F(P_Bw+1)} f_F(y) \\ & \times [F_F(z) - F_F(y)]^{K-k-2} f_F(z) dz dy dx dw \\ & + \int_{\alpha_1}^{\alpha_2} f_B(w) \int_0^{\alpha_F} \eta_k f_F(x) [F_F(x)]^{k-1} \int_{\frac{\alpha_B^{-1}w-1}{P_F}}^{\alpha_F(P_Bw+1)} \int_y^{\alpha_F(P_Bw+1)} f_F(y) \\ & \times [F_F(z) - F_F(y)]^{K-k-2} f_F(z) dz dy dx dw. \end{aligned} \quad (\text{A.15})$$

By applying (A.6) and after some manipulations,  $T_k$  can be finally represented by

$$T_k = \bar{\eta}_k I_{1;k} + \bar{\eta}_k I_{2;k}. \quad (\text{A.16})$$

2)  $k = K - 1$ : In this case, we have  $|h_{k+1}|^2 = |h_K|^2$ . Then

$$\begin{aligned} T_{K-1} = & \mathbb{P} \left\{ \alpha_B < |g|^2 < \alpha_1, |h_{K-1}|^2 < \frac{\tau(|g|^2)}{P_F}, \frac{\tau(|g|^2)}{P_F} < |h_K|^2 < \alpha_F(P_B|g|^2 + 1) \right\} \\ & + \mathbb{P} \left\{ \alpha_1 < |g|^2 < \alpha_2, |h_{K-1}|^2 < \alpha_F, \frac{\tau(|g|^2)}{P_F} < |h_K|^2 < \alpha_F(P_B|g|^2 + 1) \right\}. \end{aligned} \quad (\text{A.17})$$

The joint pdf of  $|h_{K-1}|^2$  and  $|h_K|^2$  equals

$$f_{|h_{K-1}|^2, |h_K|^2}(x, y) = \tilde{\eta}_0 f_F(x) [F_F(x)]^{K-2} f_F(y), \quad (\text{A.18})$$

where  $x \leq y$ , and  $\tilde{\eta}_0 = K(K - 1)$ . By utilizing (A.18),  $T_{K-1}$  can be further expressed as

$$\begin{aligned} T_{K-1} = & \int_{\alpha_B}^{\alpha_1} f_B(w) \int_0^{\frac{\alpha_B^{-1}w-1}{P_F}} \tilde{\eta}_0 f_F(x) [F_F(x)]^{K-2} \int_{\frac{\alpha_B^{-1}w-1}{P_F}}^{\alpha_F(P_Bw+1)} f_F(y) dy dx dw \\ & + \int_{\alpha_1}^{\alpha_2} f_B(w) \int_0^{\alpha_F} \tilde{\eta}_0 f_F(x) [F_F(x)]^{K-2} \int_{\frac{\alpha_B^{-1}w-1}{P_F}}^{\alpha_F(P_Bw+1)} f_F(y) dy dx dw. \end{aligned} \quad (\text{A.19})$$

After some manipulations,  $T_{K-1}$  can be finally represented as

$$T_{K-1} = \bar{\eta}_{K-1} I_{1;K-1} + \bar{\eta}_{K-1} I_{2;K-1}. \quad (\text{A.20})$$

### C. Calculation of $T_K$

We first rewrite  $T_K$  as

$$\begin{aligned} T_K = & \mathbb{P} \left\{ |g|^2 > \alpha_B, E_K, \log(1 + P_F|h_K|^2) < R_F \right\} \\ = & \mathbb{P} \left\{ |g|^2 > \alpha_B, |h_K|^2 < \frac{\tau(|g|^2)}{P_F}, |h_K|^2 < \alpha_F \right\}. \end{aligned} \quad (\text{A.21})$$

By utilizing (A.12),  $T_K$  can be converted to

$$T_K = \mathbb{P} \left\{ \alpha_B < |g|^2 < \alpha_1, |h_K|^2 < \frac{\tau(|g|^2)}{P_F} \right\} + \mathbb{P} \left\{ |g|^2 > \alpha_1, |h_K|^2 < \alpha_F \right\}. \quad (\text{A.22})$$

Since  $|g|^2$  and  $|h_K|^2$  are independent, we have

$$\begin{aligned} T_K &= \int_{\alpha_B}^{\alpha_1} f_B(w) \left[ F_F \left( \frac{\alpha_B^{-1}w - 1}{P_F} \right) \right]^K dw + (1 - F_B(\alpha_1)) [F_F(\alpha_F)]^K \\ &= I_{1,K} + I_{2,K} + I_4, \end{aligned} \quad (\text{A.23})$$

where the CDF of the largest order statistic  $F_{|h_K|^2}(x) = [F_F(x)]^K$  is applied.

#### D. Calculation of $T_{K+1}$

$T_{K+1}$  can be calculated following the similar way in deriving  $T_K$  as

$$\begin{aligned} T_{K+1} &= \mathbb{P} \left\{ |g|^2 < \alpha_B, \log \left( 1 + \frac{P_F |h_K|^2}{P_B |g|^2 + 1} \right) < R_F \right\} \\ &= \mathbb{P} \left\{ |g|^2 < \alpha_B, |h_K|^2 < \alpha_F (P_B |g|^2 + 1) \right\} \\ &= I_3, \end{aligned} \quad (\text{A.24})$$

where

$$I_3 = \int_0^{\alpha_B} f_B(w) [F_F(\alpha_F P_B w + \alpha_F)]^K dw. \quad (\text{A.25})$$

Finally, by combining (A.7), (A.16), (A.20), (A.23), and (A.24), we have

$$\mathcal{P}_{\text{BU}} = \sum_{k=0}^K \bar{\eta}_k I_{1;k} + \sum_{k=0}^K \bar{\eta}_k I_{2;k} + I_3 + I_4. \quad (\text{A.26})$$

Since it is quite involved to derive a closed-form expression for (A.26), an approximation is given in the first approximation of (11) by using Gaussian-Chebyshev quadrature [42].

For the case of  $\gamma_B \gamma_F \geq 1$ , after some manipulations, we have

$$\mathcal{P}_{\text{BU}} = \sum_{k=0}^K \bar{\eta}_k I_{1;k} + \sum_{k=0}^K \bar{\eta}_k I_{2;k} (\alpha_2 \mapsto \infty) + I_3, \quad (\text{A.27})$$

where  $I_{2;k} (\alpha_2 \mapsto \infty)$  denotes the expression of replacing  $\alpha_2$  in  $I_{2;k}$  with  $\infty$ . Next we show how to find the exact expression of  $I_{2;k} (\alpha_2 \mapsto \infty)$ . First, we can rewrite (2) as

$$F_F(x) \approx -\frac{1}{2} \sum_{l=0}^L \Psi_l e^{-\mu_l x}, \quad (\text{A.28})$$

where  $\Psi_0 = -2$  and  $\mu_0 = 0$ . Then, by applying binomial theorem,  $I_{2;k}(\alpha_2 \mapsto \infty)$  becomes

$$I_{2;k}(\alpha_2 \mapsto \infty) = [F_F(\alpha_F)]^k \int_{\alpha_1}^{\infty} f_B(w) \sum_{m=0}^{K-k} \binom{K-k}{m} (-1)^m \times F_F(\alpha_F P_B w + \alpha_F)^{K-k-m} F_F\left(\frac{\alpha_B^{-1} w - 1}{P_F}\right)^m dw. \quad (\text{A.29})$$

Based on (A.28), we first derive the following expression

$$\begin{aligned} [F_F(x)]^M &\approx \left( -\frac{1}{2} \sum_{l=0}^L \Psi_l e^{-\mu_l x} \right)^M \\ &\approx \left( -\frac{1}{2} \right)^M \sum_{\sum_{l=0}^L p_l = M} \binom{M}{p_0, \dots, p_L} \left( \prod_{l=0}^L \Psi_l^{p_l} \right) e^{-\sum_{l=0}^L p_l \mu_l x}. \end{aligned} \quad (\text{A.30})$$

Substituting (A.30) into (A.29),  $I_{2;k}(\alpha_2 \mapsto \infty)$  can be calculated as

$$\begin{aligned} I_{2;k}(\alpha_2 \mapsto \infty) &= \frac{[F_F(\alpha_F)]^k}{D_0 + D_1} \int_{\alpha_1}^{\infty} \sum_{n=1}^N \Phi_n c_n e^{-c_n w} \sum_{m=0}^{K-k} \binom{K-k}{m} (-1)^m \left( -\frac{1}{2} \right)^{K-k-m} \\ &\quad \times \sum_{\sum_{l=0}^L p_l = K-k-m} \binom{K-k-m}{p_0, \dots, p_L} \left( \prod_{l=0}^L \Psi_l^{p_l} \right) e^{-\sum_{l=0}^L p_l \mu_l (\alpha_F P_B w + \alpha_F)} \\ &\quad \times \left( -\frac{1}{2} \right)^m \sum_{\sum_{l=0}^L q_l = m} \binom{m}{q_0, \dots, q_L} \left( \prod_{l=0}^L \Psi_l^{q_l} \right) e^{-\sum_{l=0}^L q_l \mu_l \left( \frac{\alpha_B^{-1} w - 1}{P_F} \right)} dw \\ &= \left( -\frac{1}{2} \right)^{K-k} \frac{[F_F(\alpha_F)]^k}{D_0 + D_1} \sum_{n=1}^N \Phi_n c_n \sum_{m=0}^{K-k} \binom{K-k}{m} (-1)^m \\ &\quad \times \sum_{\sum_{l=0}^L p_l = K-k-m} \binom{K-k-m}{p_0, \dots, p_L} \sum_{\sum_{l=0}^L q_l = m} \binom{m}{q_0, \dots, q_L} \left( \prod_{l=0}^L \Psi_l^{p_l+q_l} \right) \\ &\quad \times e^{\sum_{l=0}^L (q_l \mu_l P_F^{-1} - p_l \mu_l \alpha_F)} \int_{\alpha_1}^{\infty} e^{-[\sum_{l=0}^L (p_l \mu_l \alpha_F P_B + q_l \mu_l P_F^{-1} \alpha_B^{-1}) + c_n] w} dw \\ &= H_{2;k}. \end{aligned} \quad (\text{A.31})$$

Finally, by applying Gaussian-Chebyshev quadrature to  $I_{1;k}$  and  $I_3$ , and substituting the result of (A.31) to  $I_{2;k}$  in (A.27), we can obtain the second approximation of (11). This completes the proof of Theorem 1.

## APPENDIX B PROOF OF COROLLARY 1

The high SNR approximation of  $\mathcal{P}_{\text{BU}}$  is calculated by using (A.26) for the case  $\gamma_B \gamma_F < 1$ . First, we note that, when  $x \rightarrow 0$  and applying  $e^{-x} \approx 1 - x$ , the CDF of the GF users' unordered

channel gains in (2) can be approximated as

$$F_F(x) \approx \frac{1}{2} \sum_{l=1}^L \Psi_l \mu_l x = S_F x, \quad (\text{A.32})$$

where  $S_F = \frac{1}{2} \sum_{l=1}^L \Psi_l \mu_l$ . Similarly, when  $y \rightarrow 0$ , the pdf of the GB user's channel gain can be approximated as

$$f_B(y) \approx \frac{1}{D_0 + D_1} \sum_{n=1}^N \Phi_n c_n (1 - c_n y). \quad (\text{A.33})$$

When  $P_B = P_F \rightarrow \infty$ , we have  $\alpha_1 = (1 + \gamma_F) \alpha_B \rightarrow 0$ . And when  $w \leq \alpha_1$ , we have  $\alpha_F P_B w + \alpha_F \leq \gamma_F \alpha_1 + \alpha_F \rightarrow 0$  and  $\frac{\alpha_B^{-1} w - 1}{P_F} \leq \alpha_F \rightarrow 0$ . Therefore, by applying (A.32) and (A.33), the high SNR approximation of  $I_{1;k}$  in (A.26) can be derived as

$$\begin{aligned} I_{1;k} &\approx \int_{\alpha_B}^{\alpha_1} \frac{S_F^k}{D_0 + D_1} \sum_{n=1}^N \Phi_n c_n (1 - c_n w) \left( \frac{\alpha_B^{-1} w - 1}{P_F} \right)^k \\ &\quad \times \left[ S_F (\alpha_F P_B w + \alpha_F) - S_F \left( \frac{\alpha_B^{-1} w - 1}{P_F} \right) \right]^{K-k} dw \\ &\approx S_B S_F^K \int_{\alpha_B}^{\alpha_1} \left( \gamma_F w - \gamma_B^{-1} w + \frac{\gamma_F + 1}{P_F} \right)^{K-k} (\gamma_B^{-1} w - P_F^{-1})^k dw \\ &= S_B S_F^K \int_{\alpha_B}^{\alpha_1} \sum_{i=0}^{K-k} \binom{K-k}{i} \left( \frac{\gamma_F + 1}{P_F} \right)^{K-k-i} \\ &\quad \times (\gamma_F w - \gamma_B^{-1} w)^i \sum_{j=0}^k \binom{k}{j} (\gamma_B^{-1} w)^{k-j} (-1)^j P_F^{-j} dw \\ &= \vec{I}_{1;k}. \end{aligned} \quad (\text{A.34})$$

When  $P_B = P_F \rightarrow \infty$ , we have  $\alpha_2 = \frac{\alpha_B(\gamma_F+1)}{1-\gamma_B\gamma_F} \rightarrow 0$ . If  $w \leq \alpha_2$ , we have  $\alpha_F P_B w + \alpha_F \rightarrow 0$  and  $\frac{\alpha_B^{-1} w - 1}{P_F} \rightarrow 0$ . Similarly, by substituting (A.32) and (A.33) into  $I_{2;k}$  in (A.26), we have

$$I_{2;k} \approx \int_{\alpha_1}^{\alpha_2} \frac{S_F^K}{D_0 + D_1} \sum_{n=1}^N \Phi_n c_n (1 - c_n w) \alpha_F^k \left( \gamma_F w + \alpha_F - \frac{\alpha_B^{-1} w - 1}{P_F} \right)^{K-k} dw. \quad (\text{A.35})$$

After some algebraic manipulations, the high SNR approximation of  $I_{2;k}$  becomes  $\vec{I}_{2;k}$ . Following the same steps as deriving the high SNR approximation of  $I_{1;k}$ , the high SNR approximations of  $I_3$  and  $I_4$  can be calculated as  $\vec{I}_3$  and  $\vec{I}_4$ , respectively. Substituting the above results into (A.26), we can obtain the first equation of (17).

According to the proof of Theorem 1, for the case  $\gamma_B \gamma_F \geq 1$ , we only need to find the high SNR approximation of  $I_{2;k}(\alpha_2 \mapsto \infty)$ . When  $P_B = P_F \rightarrow \infty$ , we have the following two approximations:  $\sum_{l=0}^L (q_l \mu_l P_F^{-1} - p_l \mu_l \alpha_F) \rightarrow 0$  and  $\left[ \sum_{l=0}^L (p_l \mu_l \alpha_F P_B + q_l \mu_l P_F^{-1} \alpha_B^{-1}) + c_n \right] \alpha_1 \rightarrow 0$ .

Substituting the above two approximations into (A.31) and applying  $e^{-x} \approx 1 - x$ , we can find that the high SNR approximation of  $I_{2;k}(\alpha_2 \mapsto \infty)$  is  $\vec{H}_{2;k}$ . Then we can derive the second equation of (17) straightforwardly. The proof of Corollary 1 is complete.

### APPENDIX C PROOF OF THEOREM 2

Firstly, we find that  $\Delta_1$  can be rewritten as

$$\Delta_1 = \mathbb{P} \left\{ |g|^2 < \alpha_B, |h|^2 < \alpha_F (P_B |g|^2 + 1) \right\}. \quad (\text{A.36})$$

Since the channels of the GB user  $g$  and the admitted GF user  $h$  are independent, by substituting (4) and (7) into (A.36),  $\Delta_1$  can be approximated as

$$\Delta_1 \approx \int_0^{\alpha_B} \Xi_2 \left[ 1 - e^{-\mu_l \alpha_F (P_B w + 1)} \right]^K c_n e^{-c_n w} dw. \quad (\text{A.37})$$

By applying binomial theorem,  $\Delta_1$  can be further approximated as

$$\begin{aligned} \Delta_1 &\approx \Xi_2 c_n \sum_{k=0}^K \binom{K}{k} (-1)^k \int_0^{\alpha_B} e^{-k \mu_l \alpha_F (P_B w + 1) - c_n w} dw \\ &= \frac{\Xi_1 c_n}{\Theta_1} e^{-k \mu_l \alpha_F} (1 - e^{-\Theta_1 \alpha_B}). \end{aligned} \quad (\text{A.38})$$

For  $\Delta_2$ , it can be expressed as

$$\Delta_2 = \mathbb{P} \left\{ |g|^2 > \alpha_B, \frac{\tau(|g|^2)}{P_F} < |h|^2 < \alpha_F (P_B |g|^2 + 1) \right\}. \quad (\text{A.39})$$

Applying the hidden constraint in (A.2), we calculate  $\Delta_2$  by considering two cases. For the first case of  $\gamma_B \gamma_F < 1$ ,  $\Delta_2$  becomes

$$\Delta_2 = \mathbb{P} \left\{ \alpha_B < |g|^2 < \alpha_2, \frac{\tau(|g|^2)}{P_F} < |h|^2 < \alpha_F (P_B |g|^2 + 1) \right\}. \quad (\text{A.40})$$

By applying (4) and (7), and substituting  $\tau(|g|^2) = \alpha_B^{-1} |g|^2 - 1$ ,  $\Delta_2$  can be approximated as

$$\begin{aligned} \Delta_2 &\approx \int_{\alpha_B}^{\alpha_2} \left[ (1 - e^{-\mu_l \alpha_F (P_B w + 1)})^K - (1 - e^{-\frac{\mu_l (w - \alpha_B)}{P_F \alpha_B}})^K \right] \\ &\quad \times \frac{1}{2} \sum_{l=1}^L \Psi_l \frac{1}{D_1 + D_0} \sum_{n=1}^N \Phi_n c_n e^{-c_n w} dw. \end{aligned} \quad (\text{A.41})$$

After some manipulations, the approximation of  $\Delta_2$  can be simplified as

$$\Delta_2 \approx \frac{\Xi_1 c_n}{\Theta_1} e^{-k \mu_l \alpha_F} (e^{-\Theta_1 \alpha_B} - e^{-\Theta_1 \alpha_2}) - \frac{\Xi_1 c_n}{\Theta_2} e^{\frac{k \mu_l}{P_F}} (e^{-\Theta_2 \alpha_B} - e^{-\Theta_2 \alpha_2}). \quad (\text{A.42})$$

For the second case of  $\gamma_B \gamma_F \geq 1$ ,  $\Delta_2$  becomes

$$\Delta_2 = \mathbb{P} \left\{ |g|^2 > \alpha_B, \frac{\tau(|g|^2)}{P_F} < |h|^2 < \alpha_F (P_B |g|^2 + 1) \right\}. \quad (\text{A.43})$$

Similarly, by substituting (4) and (7), and after some manipulations,  $\Delta_2$  can be approximated as

$$\Delta_2 \approx \Xi_2 c_n \sum_{k=0}^K \binom{K}{k} (-1)^k e^{-k\mu_l \alpha_F} \frac{e^{-\Theta_1 \alpha_B}}{\Theta_1} - \Xi_2 c_n \sum_{k=0}^K \binom{K}{k} (-1)^k e^{-\frac{k\mu_l}{P_F}} \frac{e^{-\Theta_2 \alpha_B}}{\Theta_2}. \quad (\text{A.44})$$

For  $\Delta_3$ , by applying (A.12), it can be rewritten as

$$\Delta_3 = \mathbb{P} \left\{ \alpha_B < |g|^2 < \alpha_1, |h|^2 < \frac{\tau(|g|^2)}{P_F} \right\} + \underbrace{\mathbb{P} \left\{ |g|^2 > \alpha_1, |h|^2 < \alpha_F \right\}}_{A_1}. \quad (\text{A.45})$$

By applying (3) and (7),  $A_1$  can be approximated as

$$\begin{aligned} A_1 &\approx \frac{1}{2} \left[ 1 - \frac{1}{D_1 + D_0} \sum_{n=1}^N \Phi_n (1 - e^{-c_n \alpha_1}) \right] \sum_{l=1}^L \Psi_l (1 - e^{-\mu_l \alpha_F})^K \\ &= \Xi_2 e^{-c_n \alpha_1} (1 - e^{-\mu_l \alpha_F})^K, \end{aligned} \quad (\text{A.46})$$

where the equality holds by using  $\frac{1}{D_1 + D_0} \sum_{n=1}^N \Phi_n = 1$ . Following the previous derivation procedure and considering (A.46),  $\Delta_3$  can be approximated as

$$\Delta_3 \approx \frac{\Xi_1 c_n}{\Theta_2} e^{\frac{k\mu_l}{P_F}} (e^{-\Theta_2 \alpha_B} - e^{-\Theta_2 \alpha_1}) + \Xi_2 e^{-c_n \alpha_1} (1 - e^{-\mu_l \alpha_F})^K. \quad (\text{A.47})$$

Finally, we can obtain (24) by combining (A.38), (A.42), and (A.47), and combining (A.38), (A.44), and (A.47). The proof is complete.

#### APPENDIX D PROOF OF THEOREM 3

As all the GF users' maximal transmit powers are assumed to be  $P_m$  and their channel gains are ordered as (1),  $T_0^{\text{PC}}$  can be rewritten as

$$\begin{aligned} T_0^{\text{PC}} &= \mathbb{P} \left\{ |g|^2 > \alpha_B, P_m |h_1|^2 > \tau(|g|^2), \frac{P_m |h_K|^2}{P_B |g|^2 + 1} > \tau(|g|^2), \frac{P_m |h_K|^2}{P_B |g|^2 + 1} < \gamma_F \right\} \\ &\quad + \mathbb{P} \left\{ |g|^2 > \alpha_B, P_m |h_1|^2 > \tau(|g|^2), \frac{P_m |h_K|^2}{P_B |g|^2 + 1} < \tau(|g|^2), \tau(|g|^2) < \gamma_F \right\}. \end{aligned} \quad (\text{A.48})$$

After some manipulations,  $T_0^{\text{PC}}$  can be rewritten as

$$\begin{aligned} T_0^{\text{PC}} &= \mathbb{P} \left\{ \alpha_B < |g|^2 < \alpha_1, |h_1|^2 > \frac{\tau(|g|^2)}{P_m}, \frac{P_B |g|^2 + 1}{P_m} \tau(|g|^2) < |h_K|^2 < \frac{P_B |g|^2 + 1}{P_m} \gamma_F \right\} \\ &\quad + \mathbb{P} \left\{ \alpha_B < |g|^2 < \alpha_1, |h_1|^2 > \frac{\tau(|g|^2)}{P_m}, |h_K|^2 < \frac{P_B |g|^2 + 1}{P_m} \tau(|g|^2) \right\}, \end{aligned} \quad (\text{A.49})$$

where  $\alpha_1 = \alpha_B(1 + \gamma_F)$ , and the constraint  $|g|^2 < \alpha_1$  is obtained due to  $\tau(|g|^2) < \gamma_F$  and  $\tau(|g|^2) = \alpha_B^{-1} |g|^2 - 1$ . Surprisingly, we find that the two terms in (A.49) can be combined, so

that  $T_0^{\text{PC}}$  can be further simplified as

$$T_0^{\text{PC}} = \mathbb{P} \left\{ \alpha_B < |g|^2 < \alpha_1, |h_1|^2 > \frac{\tau(|g|^2)}{P_m}, |h_K|^2 < \frac{P_B|g|^2 + 1}{P_m} \gamma_F \right\}. \quad (\text{A.50})$$

By comparing (A.50) with (A.3), we can find that  $T_0^{\text{PC}}$  is less than  $T_0$  in (A.3), since  $\alpha_F = \frac{\gamma_F}{P_F}$ ,  $P_F \leq P_m$  and  $\alpha_1 < \alpha_2$  (where  $\alpha_2 = \frac{\alpha_B(\gamma_F+1)}{1-\gamma_B\gamma_F}$  when  $\gamma_B\gamma_F < 1$ , and  $\alpha_2 = \infty$  when  $\gamma_B\gamma_F \geq 1$ ). Moreover, by comparing the calculation process from (A.1) to (A.3) with that from (A.48) to (A.50), we can also find that the constraint of  $\gamma_B\gamma_F < 1$  required for the derivation of (A.3) is not required here any more. Following the same steps of deriving (A.7), we have  $T_0^{\text{PC}} = I_{1;0}(P_F \mapsto P_m)$ .

Then,  $T_k^{\text{PC}} (1 \leq k \leq K-1)$  can be rewritten as

$$\begin{aligned} T_k^{\text{PC}} = & \mathbb{P} \left\{ |g|^2 > \alpha_B, P_m|h_k|^2 < \gamma_F, P_m|h_k|^2 < \tau(|g|^2), \right. \\ & P_m|h_{k+1}|^2 > \tau(|g|^2), \tau(|g|^2) < \frac{P_m|h_K|^2}{P_B|g|^2 + 1} < \gamma_F \left. \right\} \\ & + \mathbb{P} \left\{ |g|^2 > \alpha_B, |h_k|^2 < \frac{\tau(|g|^2)}{P_m}, |h_{k+1}|^2 > \frac{\tau(|g|^2)}{P_m}, \right. \\ & \left. P_m|h_k|^2 < \gamma_F, \frac{P_m|h_K|^2}{P_B|g|^2 + 1} < \tau(|g|^2), \tau(|g|^2) < \gamma_F \right\}. \end{aligned} \quad (\text{A.51})$$

After some algebraic operations, (A.51) can be converted to

$$\begin{aligned} T_k^{\text{PC}} = & \mathbb{P} \left\{ \alpha_B < |g|^2 < \alpha_1, |h_k|^2 < \frac{\tau(|g|^2)}{P_m}, |h_{k+1}|^2 > \frac{\tau(|g|^2)}{P_m}, \right. \\ & |h_k|^2 < \frac{\gamma_F}{P_m}, \frac{P_B|g|^2 + 1}{P_m} \tau(|g|^2) < |h_K|^2 < \frac{P_B|g|^2 + 1}{P_m} \gamma_F \left. \right\} \\ & + \mathbb{P} \left\{ \alpha_B < |g|^2 < \alpha_1, |h_k|^2 < \frac{\tau(|g|^2)}{P_m}, |h_k|^2 < \frac{\gamma_F}{P_m}, \right. \\ & |h_{k+1}|^2 > \frac{\tau(|g|^2)}{P_m}, |h_K|^2 < \frac{P_B|g|^2 + 1}{P_m} \tau(|g|^2) \left. \right\}. \end{aligned} \quad (\text{A.52})$$

Combining the two parts of (A.52) together, we have

$$\begin{aligned} T_k^{\text{PC}} = & \mathbb{P} \left\{ \alpha_B < |g|^2 < \alpha_1, |h_k|^2 < \frac{\tau(|g|^2)}{P_m}, |h_k|^2 < \frac{\gamma_F}{P_m}, \right. \\ & |h_{k+1}|^2 > \frac{\tau(|g|^2)}{P_m}, |h_K|^2 < \frac{P_B|g|^2 + 1}{P_m} \gamma_F \left. \right\}. \end{aligned} \quad (\text{A.53})$$

Since  $|g|^2 < \alpha_1$ , by applying (A.12), we can further simplify  $T_k^{\text{PC}}$  as

$$T_k^{\text{PC}} = \mathbb{P} \left\{ \alpha_B < |g|^2 < \alpha_1, |h_k|^2 < \frac{\tau(|g|^2)}{P_m}, |h_{k+1}|^2 > \frac{\tau(|g|^2)}{P_m}, |h_K|^2 < \frac{P_B|g|^2 + 1}{P_m} \gamma_F \right\}. \quad (\text{A.54})$$

By comparing (A.54) with (A.13), we can find that  $T_k^{\text{PC}}$  is no larger than the first part of  $T_k$

in (A.13), since  $\alpha_F = \frac{\gamma_F}{P_F}$  and  $P_F \leq P_m$ . Following the same lines of deriving (A.16) and (A.20),  $T_k^{PC} = I_{1;k}(P_F \mapsto P_m)$  for  $(1 \leq k \leq K-1)$ . Similarly, we have  $T_K^{PC} = I_{1;K}(P_F \mapsto P_m) + I_5$  and  $T_{K+1}^{PC} = I_3(P_F \mapsto P_m)$ .

Combining all the above results, we have

$$\mathcal{P}_{BU}^{PC} = \sum_{k=0}^K \bar{\eta}_k I_{1;k}(P_F \mapsto P_m) + I_3(P_F \mapsto P_m) + I_5. \quad (\text{A.55})$$

Similar with (11), we can obtain (34) by applying Gaussian-Chebyshev quadrature to (A.55), and the proof is complete.

## REFERENCES

- [1] J. G. Andrews, S. Buzzi, W. Choi, S. V. Hanly, A. Lozano, A. C. K. Soong and J. C. Zhang, "What will 5G be?", *IEEE J. Sel. Areas Commun.*, vol. 32, no. 6, pp. 1065-1082, Jun. 2014.
- [2] "Study on scenarios and requirements for next generation access technologies (release 14), V14.2.0," 3GPP, Sophia Antipolis, France, Rep. TR 38.913, Mar. 2017.
- [3] O. L. A. López, H. Alves, P. H. J. Nardelli, and M. Latva-Aho, "Aggregation and resource scheduling in machine-type communication networks: A stochastic geometry approach," *IEEE Trans. Wireless Commun.*, vol. 17, no. 7, pp. 4750-4765, Jul. 2018.
- [4] M. Shirvanimoghaddam, M. Dohler, and S. J. Johnson, "Massive non-orthogonal multiple access for cellular IoT: Potentials and limitations," *IEEE Commun. Mag.*, vol. 55, no. 9, pp. 55-61, Sep. 2017.
- [5] G. Durisi, T. Koch, and P. Popovski, "Toward massive, ultrareliable, and low-latency wireless communication with short packets," *Proc. IEEE*, vol. 104, no. 9, pp. 1711-1726, Aug. 2016.
- [6] Z. Dawy et al., "Toward Massive Machine Type Cellular Communications," *IEEE Wireless Commun.*, vol. 24, no. 1, pp. 120-28, Feb. 2017.
- [7] M. Gharbieh, H. ElSawy, H. Yang, A. Bader and M. Alouini, "Spatiotemporal model for uplink IoT traffic: Scheduling and random access paradox," *IEEE Trans. Wireless Commun.*, vol. 17, no. 12, pp. 8357-8372, Dec. 2018.
- [8] Y. Cui, W. Xu, Y. Wang, J. Lin and L. Lu, "Side-information aided compressed multi-user detection for up-link grant-free NOMA," *IEEE Trans. Wireless Commun.*, vol. 19, no. 11, pp. 7720-7731, Nov. 2020.
- [9] S.-Y. Lien, S.-L. Shieh, Y. Huang, B. Su, Y.-L. Hsu, and H.-Y. Wei, "5G new radio: Waveform, frame structure, multiple access, and initial access," *IEEE Commun. Mag.*, vol. 55, no. 6, pp. 64-71, Jun. 2017.
- [10] A. Bayesteh, E. Yi, H. Nikopour, and H. Bahligh, "Blind detection of SCMA for uplink grant-free multiple-access," in *Proc. Int. Symp. Wireless Commun. Systems (ISWCS)*, Aug. 2014, PP. 853-857.
- [11] M. Vaezi, Z. Ding, and H. V. Poor, *Multiple Access Techniques for 5G Wireless Networks and Beyond*. Springer Press, 2019.
- [12] Y. Yuan et al., "Nonorthogonal transmission technology in LTE evolution," *IEEE Commun. Mag.*, vol. 54, no. 7, pp. 68-74, Jul. 2016.
- [13] S. Dogan, A. Tusha, and H. Arslan, "NOMA with index modulation for uplink URLLC through grant-free access," *IEEE J. Sel. Topics Signal Process.*, vol. 13, no. 6, pp. 1249-1257, Oct. 2019.
- [14] K. Yang, N. Yang, N. Ye, M. Jia, Z. Gao and R. Fan, "Non-orthogonal multiple access: Achieving sustainable future radio access," *IEEE Commun. Mag.*, vol. 57, no. 2, pp. 116-121, Feb. 2019.
- [15] Z. Ding, R. Schober, P. Fan, and H. V. Poor, "Simple semi-GF transmission strategies assisted by non-orthogonal multiple access," *IEEE Trans. Commun.*, vol. 67, no. 6, pp. 4464-4478, Jun. 2019.
- [16] N. Zhang et al., "Uplink nonorthogonal multiple access in 5G systems," *IEEE Commun. Lett.*, vol. 20, no. 3, pp. 458-461, Mar. 2016.
- [17] Z. Yang, Z. Ding, P. Fan, and N. Al-Dahir, "A general power allocation scheme to guarantee quality of service in downlink and uplink NOMA systems," *IEEE Trans. Wireless Commun.*, vol. 15, no. 11, pp. 7244-7257, Nov. 2016.
- [18] Z. Ding, Z. Yang, P. Fan, and H. V. Poor, "On the performance of non-orthogonal multiple access in 5G systems with randomly deployed users," *IEEE Signal Process. Lett.*, vol. 21, no. 12, pp. 1501-1505, Dec. 2014.
- [19] Y. Liu, Z. Ding, M. Elkashlan, and H. V. Poor, "Cooperative non-orthogonal multiple access with simultaneous wireless information and power transfer," *IEEE J. Sel. Areas Commun.*, vol. 34, no. 4, pp. 938-953, Apr. 2016.
- [20] Z. Zhang, H. Sun, and R. Q. Hu, "Downlink and uplink non-orthogonal multiple access in a dense wireless network," *IEEE J. Sel. Areas Commun.*, vol. 35, no. 12, pp. 2771-2784, Dec. 2017.
- [21] Z. Yang, X. Lei, Z. Ding, P. Fan, and G. K. Karagiannidis, "On the uplink sum rate of SCMA system with randomly deployed users," *IEEE Wireless Commun. Lett.*, vol. 6, pp. 338-341, Jun. 2017.

- [22] Y. Zhou, V. W. Wong, and R. Schober, "Dynamic decode-and-forward based cooperative NOMA with spatially random users," *IEEE Trans. Wireless Commun.*, vol. 17, no. 5, pp. 3340–3356, May 2018.
- [23] B. Wang, L. Dai, T. Mir, and Z. Wang, "Joint user activity and data detection based on structured compressive sensing for NOMA," *IEEE Commun. Lett.*, vol. 20, no. 7, pp. 1473–1476, Jul. 2016.
- [24] Y. Du et al., "Block-sparsity-based multiuser detection for uplink grant-free NOMA," *IEEE Trans. Wireless Commun.*, vol. 17, no. 12, pp. 7894–7909, Dec. 2018.
- [25] R. Abbas, M. Shirvanimoghaddam, Y. Li and B. Vucetic, "A novel analytical framework for massive grant-free NOMA," *IEEE Trans. Commun.*, vol. 67, no. 3, pp. 2436–2449, Mar. 2019.
- [26] F. Wei, W. Chen, Y. Wu, J. Ma, and T. A. Tsiftsis, "Message-passing receiver design for joint channel estimation and data decoding in uplink grant-free SCMA systems," *IEEE Trans. Wireless Commun.*, vol. 18, no. 1, pp. 167–181, Jan. 2019.
- [27] S. M. R. Islam et al., "Power domain non-orthogonal multiple access (NOMA) in 5G systems: Potentials and challenges," *IEEE Commun. Surveys Tuts.*, vol. 19, no. 2, pp. 721–742, 2nd Quart., 2017.
- [28] L. Dai, B. Wang, Z. Ding, Z. Wang, S. Chen, and L. Hanzo, "A survey of non-orthogonal multiple access for 5G," *IEEE Commun. Surveys Tuts.*, vol. 20, no. 3, pp. 2294–2323, 3rd Quart., 2018.
- [29] Z. Ding, X. Lei, G. K. Karagiannidis, R. Schober, J. Yuan, and V. K. Bhargava, "A survey on non-orthogonal multiple access for 5G networks: Research challenges and future trends," *IEEE J. Sel. Areas Commun.*, vol. 35, no. 10, pp. 2181–2195, Oct. 2017.
- [30] M. Elbayoumi, M. Kamel, W. Hamouda and A. Youssef, "NOMA-assisted machine-type communications in UDN: State-of-the-art and challenges," *IEEE Commun. Surveys Tuts.*, vol. 22, no. 2, pp. 1276–1304, 2nd Quart. 2020.
- [31] M. B. Shahab, R. Abbas, M. Shirvanimoghaddam and S. J. Johnson, "Grant-free non-orthogonal multiple access for IoT: A survey," *IEEE Commun. Surveys Tuts.*, vol. 22, no. 3, pp. 1805–1838, 3rd Quart., 2020.
- [32] N. Jayanth, P. Chakraborty, M. Gupta and S. Prakriya, "Performance of semi-grant free uplink with non-orthogonal multiple access," in *Proc. IEEE 31th Annu. Int. Symp. Pers., Indoor, Mobile Radio Commun. (PIMRC)*, Aug. 2020, pp. 1–6.
- [33] C. Zhang, Z. Qin, Y. Liu, and K. K. Chai, "Semi-GF uplink NOMA with contention control: A stochastic geometry model," in *Proc. IEEE Int. Conf. Commun. (ICC)*, Jul. 2020, pp. 1–6.
- [34] C. Zhang, Y. Liu, W. Yi, Z. Qin, and Z. Ding, "Semi-grant-free NOMA: Ergodic rates analysis with random deployed users," *IEEE Wireless Commun. Lett.*, doi: 10.1109/LWC.2020.3034725.
- [35] Z. Yang et al., "Adaptive power allocation for uplink non-orthogonal multiple access with semi-grant-free transmission," *IEEE Wireless Commun. Lett.*, vol. 9, no. 10, pp. 1725–1729, Oct. 2020.
- [36] Z. Ding, R. Schober, and H. V. Poor, "A new QoS-guarantee strategy for NOMA assisted semi-GF transmission," Apr. 2020. [Online]. Available: <https://arxiv.org/abs/2004.12997>
- [37] Z. Ding, R. Schober, and H. V. Poor, "Unveiling the importance of SIC in NOMA systems: Part I - state of the art and recent findings," *IEEE Commun. Lett.*, vol. 24, no. 11, pp. 2373–2377, Nov. 2020.
- [38] H. Jin et al., "Fundamental limits of CDF-based scheduling: Throughput, fairness, and feedback overhead," *IEEE/ACM Trans. Netw.*, vol. 23, no. 3, pp. 894–907, Jun. 2015.
- [39] D. Park, H. Seo, H. Kwon, and B. G. Lee, "Wireless packet admitting based on the cumulative distribution function of user transmission rate," *IEEE Trans. Commun.*, vol. 53, no. 11, pp. 1919–1929, Nov. 2005.
- [40] M. Haenggi, *Stochastic Geometry for Wireless Networks*. Cambridge, U.K.: Cambridge Univ. Press, 2012.
- [41] H. Lu, X. Xie, Z. Shi, and J. Cai, "Outage performance of CDF-based scheduling in downlink and uplink NOMA systems," *IEEE Trans. Veh. Technol.*, DOI: 10.1109/TVT.2020.3031367.
- [42] E. Hildebrand, *Introduction to Numerical Analysis*. New York, NY, USA: Dover, 1987.
- [43] Q. Zhao and L. Tong, "Opportunistic carrier sensing for energy-efficient information retrieval in sensor networks," *EURASIP J. Wireless Commun. Netw.*, vol. 2, pp. 231–241, Apr. 2005.
- [44] A. Bletsas, A. Khisti, D. P. Reed, and A. Lippman, "A simple cooperative diversity method based on network path selection," *IEEE J. Sel. Areas Commun.*, vol. 24, no. 3, pp. 659–672, Mar. 2006.
- [45] H. A. David and H. N. Nagaraja, *Order Statistics*. John Wiley, New York, 3rd ed., 2003.